NAVAL POSTGRADUATE SCHOOL
Monterey, California

THESIS

NUCLEATE POOL-BOILING
OF R-114 REFRIGERANT AND OIL MIXTURES
FROM WATER-HEATED ENHANCED SURFACES

by

Stephen M. McManus

June 1986

Thesis Advisor: P. J. Marto
Co-Advisor: A. S. Wanniarchchi

UNCLASSIFIED
SECURITY CLASSIFICATION OF THIS PAGE

REPORT DOCUMENTATION PAGE

1a REPORT SECURITY CLASSIFICATION: UNCLASSIFIED	1b. RESTRICTIVE MARKINGS
2a SECURITY CLASSIFICATION AUTHORITY	3 DISTRIBUTION / AVAILABILITY OF REPORT: Approved for public release; distribution unlimted.
2b DECLASSIFICATION / DOWNGRADING SCHEDULE	
4 PERFORMING ORGANIZATION REPORT NUMBER(S)	5 MONITORING ORGANIZATION REPORT NUMBER(S)
6a. NAME OF PERFORMING ORGANIZATION: Naval Postgraduate School; 6b OFFICE SYMBOL (If applicable): Code 69	7a. NAME OF MONITORING ORGANIZATION: Naval Postgraduate School
6c. ADDRESS (City, State, and ZIP Code): Monterey, California 93943-5000	7b. ADDRESS (City, State, and ZIP Code): Monterey, California 93943-5000
8a NAME OF FUNDING / SPONSORING ORGANIZATION: David W. Taylor NSRDC; 8b. OFFICE SYMBOL (If applicable)	9 PROCUREMENT INSTRUMENT IDENTIFICATION NUMBER
8c. ADDRESS (City, State, and ZIP Code): Annapolis, Maryland 21402	10 SOURCE OF FUNDING NUMBERS: PROGRAM ELEMENT NO; PROJECT NO; TASK NO; WORK UNIT ACCESSION NO

11 TITLE (Include Security Classification)
Nucleate Pool-Boiling of R-114 Refrigerant and Oil Mixtures from Water-Heated Enhanced Surfaces

12 PERSONAL AUTHOR(S)
McManus, Stephen, M.

13a TYPE OF REPORT	13b TIME COVERED	14 DATE OF REPORT (Year, Month, Day)	15 PAGE COUNT
Master's Thesis	FROM ______ TO ______	1986, June	99

16 SUPPLEMENTARY NOTATION

17 COSATI CODES			18 SUBJECT TERMS (Continue on reverse if necessary and identify by block number)
FIELD	GROUP	SUB-GROUP	Nucleate Pool-Boiling, Water-Heated Tubes, Enhanced Surfaces.

19 ABSTRACT (Continue on reverse if necessary and identify by block number)

Heat-transfer measurements were made for a single, water-heated tube in a pool of R-114 to simulate operating conditions of a water chiller. Data were obtained for a smooth copper tube, and for two commercially available tubes: a spirally roped copper-nickel tube with a porous coating; and a copper tube with a structured outer surface and a multiple-start helical ridged inner surface. Measurements were made for refrigerant-oil mixtures at oil concentrations from 0 to 6 mass percent with a boiling pool temperature of 13.8 °C. Results for the two enhanced tubes with and without oil are compared to the smooth tube data. Enhancement factors for the overall heat-transfer coefficient were 4.0 and 3.6 for the structured surface and porous-coated tubes, respectively, in pure refrigerant and at a water velocity of 2 m/s. For these same conditions the enhancement factors

(Cont next page)

20 DISTRIBUTION / AVAILABILITY OF ABSTRACT: ☒ UNCLASSIFIED/UNLIMITED ☐ SAME AS RPT ☐ DTIC USERS	21 ABSTRACT SECURITY CLASSIFICATION: Unclassified
22a NAME OF RESPONSIBLE INDIVIDUAL: P. J. Marto	22b TELEPHONE (Include Area Code): (408) 646-2586; 22c OFFICE SYMBOL: 69 Mx

DD FORM 1473, 84 MAR 83 APR edition may be used until exhausted. All other editions are obsolete

SECURITY CLASSIFICATION OF THIS PAGE

Unclassified

19. (cont)
for the out-side heat-transfer coefficient were 14.6 and 6.4 for the porous-coated and structured surface tubes, respectively.

Approved for public release; distribution is unlimited.

Nucleate Pool-Boiling of R-114 Refrigerant and Oil Mixtures from Water-Heated Enhanced Surfaces

by

Stephen M. McManus
Lieutenant, United States Navy
B.S.Ch.E., University of New Mexico, 1979

Submitted in partial fulfillment of the requirements for the degree of

MASTER OF SCIENCE IN MECHANICAL ENGINEERING

from the

NAVAL POSTGRADUATE SCHOOL
June 1986

ABSTRACT

Heat-transfer measurements were made for a single, water-heated tube in a pool of R-114 to simulate operating conditions of a water chiller. Data were obtained for a smooth copper tube, and for two commercially available tubes: a spirally roped copper-nickel tube with a porous coating; and a copper tube with a structured outer surface and a multiple-start helical ridged inner surface. Measurements were made for refrigerant-oil mixtures at oil concentrations from 0 to 6 mass percent with a boiling pool temperature of 13.8 °C. Results for the two enhanced tubes with and without oil are compared to the smooth tube data. Enhancement factors for the overall heat-transfer coefficient were 4.0 and 3.6 for the structured surface and porous-coated tubes, respectively, in pure refrigerant and at a water velocity of 2 m/s. For these same conditions the enhancement factors for the outside heat-transfer coefficient were 14.6 and 6.4 for the porous-coated and structured surface tubes, respectively.

TABLE OF CONTENTS

LIST OF TABLES

LIST OF FIGURES

ACKNOWLEDGEMENTS

The author wishes to express his appreciation to Dr. Paul J. Marto and Dr. A. S. Wanniarchchi for their advice, guidance, and enthusiastic support towards the completion of this thesis.

The author also expresses his sincere gratitude to his wife, Kay, and children, Alicia and James, for their patience with the long hours and frustrations inherent in such an endeavor.

I. INTRODUCTION

Recent developments in boiling surfaces have shown considerable enhancements in heat transfer performance. The worldwide literature on enhanced heat transfer contains over 3000 published technical papers and reports [Ref. 1: p. 81]. This increased interest in heat transfer augmentation is the result of incentives for energy and material savings. One effective way to improve the heat transfer is by using passive augmentation.

Passive augmentation uses fine-scale alteration of surfaces, both external and internal [Ref. 1: p. 82]. These surfaces may consist of either an applied porous coating or fins deformed in various ways to provide a large number of reentrant cavities on external surfaces. Methods of internal enhancement include insert devices, forged fins, or deformation of the surface (i.e., spirally roped or corrugated tube). The use of such surfaces can lead to considerable reduction in the size and weight of heat-transfer equipment. The reductions may lead to smaller capital costs or operating costs or both.

Of particular interest, in naval applications, is the reduction in the size of water chillers in refrigeration systems. While a number of investigations are currently in progress, the theoretical treatment of the boiling performance of various tubes is almost impossible owing to the very complicated mechanisms involved. The degree of difficulty increases with the presence of oil in the refrigerant liquid. In general, refrigeration systems with oil-lubricated, hermetically sealed compressors contain small mass percents of oil in the refrigerant liquid. Therefore, reliable data covering a wide variety of operating conditions for various refrigerants and different boiling

surfaces is essential to further develop more compact and efficient evaporators.

Most of the experiments on enhanced boiling surfaces reported in the literature have used electrically heated tubes. The difficulties associated with these tubes, especially during the instrumentation stage, raise questions as to the reliability of the data as described by Wanniarchchi et al [Ref. 2: p. 14]. Despite the precautions taken to minimize contact resistance, it may still be present between the thermocouple locations and the outer boiling surface. Another area of doubt, described by Wanniarchchi et al. [Ref. 2: p. 14], is the nonuniform heat fluxes generated by commercially available electrical heaters. Additionally, in order to use an electrical heated tube, the inside surface of the tube must be smooth, or any internal enhancement must be bored out. This is disadvantageous as designers would be interested in knowing the overall heat-transfer coefficient. Most industrial experiments use 2-to 3-meter-long tubes with warm water flowing inside them. While the information generated from these experiments closely approximate actual evaporators, compared to electrical heated tubes, the large water temperature drop from inlet to exit (up to 5 K) may make it difficult to study the details of the boiling process.

The type of refrigerant selected will also influence the design of evaporators. R-114, a moderate-pressure refrigerant, is receiving more attention, in particular for naval applications. Advantages to using R-114 include: (a) it belongs to the refrigerant group with the lowest toxicity, (b) it is very stable with temperature, and (c) it has a fairly large value for the energy transfer per unit volume of vapor (i.e., $E_v = h_{fg}/v_g$) [Ref. 3: pp. 281-291]. The advantages of the first two items are clear. The third item is advantageous since a higher value for E_v means lower

pressure drop through the refrigerant piping for a specified heat duty. As the normal boiling point of the type of refrigerant increases, the E_v value increases. R-11, R-113, R-114, and R-22 have E_v values in increasing order. R-114 may be preferable to R-11 and R-113 due to the higher E_v value and preferable to R-22 due to the ability to use lighter components in the refrigeration loop.

Based on the above discussion, the major objective of the present investigation was to study the boiling performance of two commercially available tubes, a porous-coated tube and a mechanically structured surface, in comparison with a smooth tube for the following conditions: (a) tubes are water-heated, (b) boiling fluid is R-114 with 0, 1, 2, and 6 percent by mass oil, and (c) boiling temperature is 13.8 °C.

II. BACKGROUND

A. NUCLEATE BOILING

When the temperature of a boiling surface exceeds the saturation temperature of a fluid by a few degrees, nucleate boiling occurs. The difference between the boiling surface and saturation temperature is the amount of wall superheat. Dougherty [Ref. 4: p. 175] defined pool-boiling as vaporization occurring under the following conditions: (1) liquid depth >> the bubble diameter, (2) there is negligible effect on heat transfer due to low or no externally imposed velocity of the fluid, and (3) the bubbles move away from the boiling surface due to a force field. With the above conditions, the heat flow can be expressed as:

$$h = \frac{Q}{A\Delta T} \tag{2.1}$$

A description of the boiling mechanism is given by Chongrungreong and Sauer [Ref. 5: p. 701]. A thin layer of superheated liquid is formed adjacent to the boiling surface. Bubbles nucleate in this thin layer and grow from preferred spots on the boiling surface. It is assumed that the primary resistance to heat transfer is within the thin liquid layer. The height of the liquid in the boiling container is not a primary variable, but the liquid properties should be controlled. However, large flooded evaporators may experience a significant "submergence effect" from the liquid head.

B. EXTERNAL SURFACE ENHANCEMENT

For smooth heating surfaces, bubbles nucleate at various scratches and cavities on the surface. Fujii stated that the number of active sites increases as the heat flux increases

[Ref. 6: p. 48]. Webb [Ref. 7: p. 46] stated that the ability to enhance the nucleate boiling coefficient by applying some type of roughness has been known for over 50 years.

Presently, there are two major types of commercially developed roughnesses: (1) porous coating and (2) various fins and surfaces with reentrant cavities [Ref. 8: p. 24]. The first type of roughness is a sintered particle coating, usually copper or aluminum. Figure 2.1 shows a schematic and a photomicrograph of a porous coating. The small reentrant cavities are interconnected by substrate tunnels. The surface reduces the required superheat for vapor generation by entrapping a high density of relatively large vapor nuclei in the cavities contained within the porous coating [Ref. 8: p. 24]. As described by Webb [Ref. 7: p. 58], researchers found that a critical pore size not a particle size governs the number of nucleation sites. Large pores are required for liquids with high surface tension and high thermal conductivity, while small pores work best for liquids with low surface tension and low thermal conductivity (i.e., refrigerants). Czikk and O'Neill [Ref. 9: p. 53] developed correlations to include the effects of different pore sizes of porous-coatings. They concluded that there were two resistances to heat transfer for these coatings: a nucleation superheat related to bubble diameter; and a conduction superheat controlled by the liquid film separating the vapor bubbles from the metal matrix. Carnavos [Ref. 10: pp. 106-108] found that a porous coating resulted in a 700-800 percent better heat-transfer coefficient than a smooth surface in a pool of R-11. Czikk [Ref. 11: p. 98] also found increased performance of the porous-coated tubes used in his 20-ton water-chiller experiment.

Structured fins or surfaces form reentrant cavities of various geometries. Figure 2.2 is shows an example of a

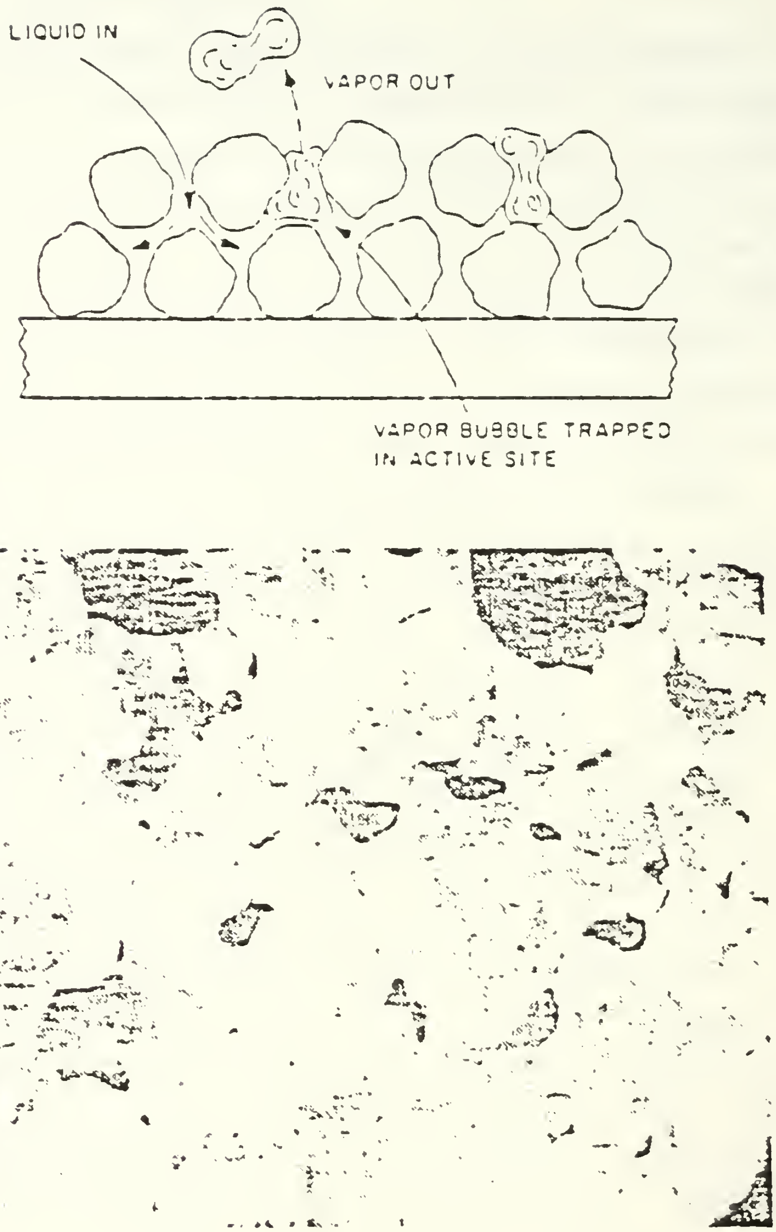

Figure 2.1. Schematic and Scanning Electron Micrograph (500x) of High Flux Surface (from Ref. 8).

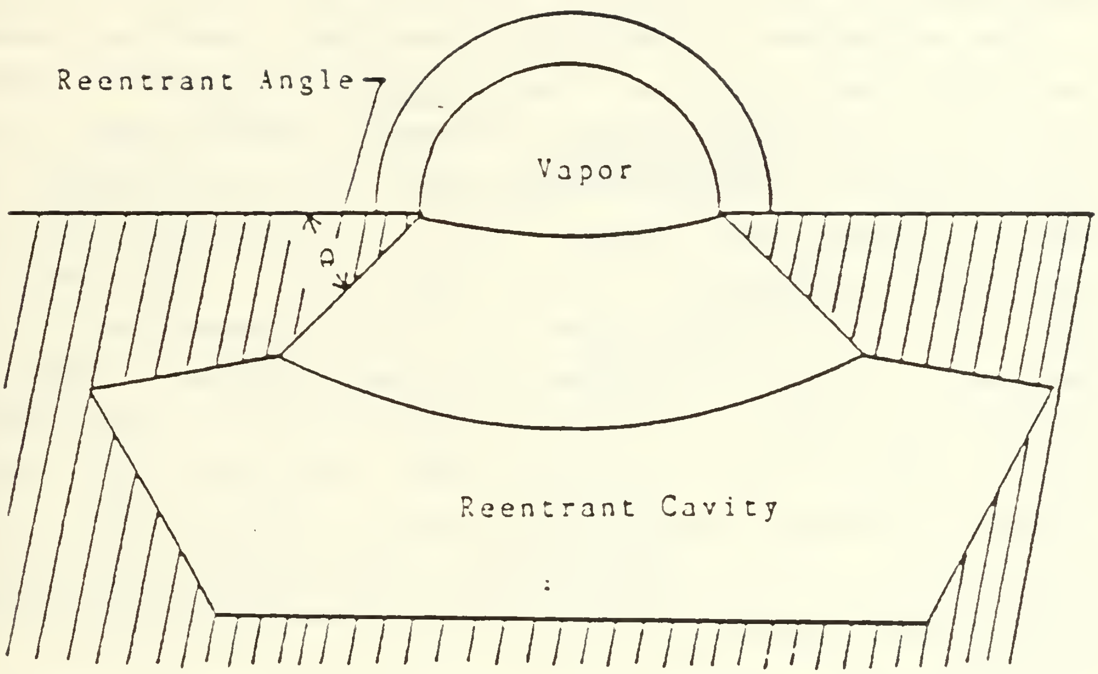

Figure 2.2. Schematic of Manufactured Reentrant Cavity (from Ref. 8).

manufactured reentrant cavity. These reentrant cavities act as stable nucleation sites, which enhances the heat transfer. The nucleation site, to remain active, is dependent on the mouth diameter falling within a critical range and shape with a maximum reentrant angle. This range is a function of the fluid properties. The cost of these surfaces, presently, are not significantly higher than the cost for smooth tubes and they dramatically improve boiling performance compared to the smooth tubes.

The mechanisms by which the reentrant cavities operate are complicated. Previous research concluded that the combination of bubble evaporation, thermal boundary-layer stripping and bubble agitation controlled the heat transfer from smooth surfaces [Ref. 12: p. 192]. In contrast, different experiments conducted by Arshad [Ref. 12: p. 192] and Arai [Ref. 13: p. 37] show that thin film evaporation in the reentrant cavity controlled the heat-transfer mechanism. Bubbles were formed by vapor exiting cavities as the liquid-vapor interface of the thin film contacted the cavity surface. Surface tension holds most of the liquid on the cavity walls. Ayub [Ref. 14: p. 64] showed this similar "thermosiphon mechanism" with his experiments using enhanced surfaces.

Nakayama [Ref. 15: p. 37] gives a fairly detailed description of a physical model undergoing this bubble growth mechanism. Figure 2.3 shows the three major phases of bubble growth. Phase I consists of a pressure buildup in the tunnel by evaporation of liquid held in corners and continues until the meniscus reaches a hemispherical shape of radius $r_o = d_o/2$ (where d_o is the mouth diameter of the reentrant cavity). In Phase II, the meniscus grows faster at some pores than at others. The Phase I pressure buildup is reduced as the vapor enters the growing bubbles. The meniscus at inactive pores does not grow due to this vapor

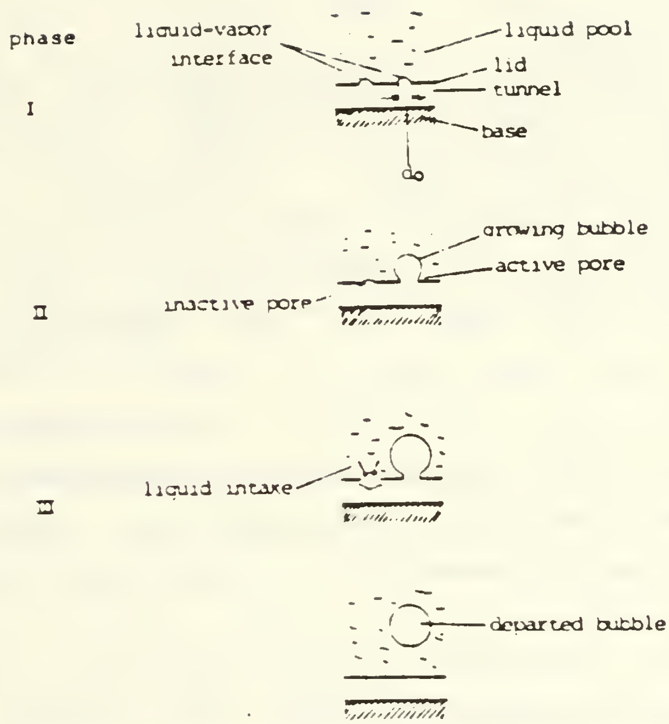

Figure 2.3. Physical Model of Bubble Mechanism (from Ref. 15).

pressure reduction. Initially, the bubble expands under the high internal pressure, while lacer expansion is controlled by the receding liquid inertia around the bubble. Phase III is termed the liquid intake phase with liquid flowing into the tunnel through inactive pores. This flow is over a short interval of pressure depression which occurs as the pressure of the bubble and tunnel is lower than the pool pressure. The bubble leaves the pore and new meniscus formation closes off the pore, ending this phase and returning the cycle to Phase I.

C. EFFECTS OF OIL

The introduction of oil into the pure refrigerant, in general, causes a decrease in the boiling coefficient as the oil concentration increases. The effects of oil on the mixture are theoretically complicated as most empirical equations relating physical properties are derived form experimental data and not from theoretical equations. Various empirical equations are cited by Chongrungreong and Sauer [Ref. 5: pp. 703-705]. Yet, Jensen and Jackman [Ref. 16: p. 184] showed that the correlation developed by Chongrungreong and Sauer appeared to overpredict as oil concentrations increased due to poor prediction of the mixture viscosity.

Predictive equations were developed by Jensen and Jackman [Ref. 16: pp. 186-187] for density, viscosity, surface tension and specific heat for pure R-113, pure oil, and R-113-oil mixtures. These equations are:

$$\frac{1}{\rho_m} = \frac{C_c}{\rho_{ol}} + \frac{1-C_c}{\rho_{rl}} \tag{2.2}$$

$$\mu_m = \mu_r \exp\left[C_c\left(\frac{\mu_o}{\mu_r}\right)^{0.3}\right] \tag{2.3}$$

$$\sigma_m = \sigma_r + (\sigma_o - \sigma_r) C_c^{0.5} \tag{2.4}$$

$$c_{p_m} = (1 - C_c) c_{p_{rl}} + c_{p_{ol}} \tag{2.5}$$

These equations are based on a physical model shown in Figure 2.4 developed by Jensen and Jackman [Ref. 16: pp. 187-188]. The model shows a bubble growing on a heated surface as the refrigerant evaporates from the superheated liquid phase into the bubble interior. Due to the less volatile nature of the oil in the mixture, it does not evaporate into the bubble, but, remains at the liquid-vapor interface. The decrease in the rate of bubble growth is due to the decrease of oil diffusion into the liquid mixture and the decrease of refrigerant through the oil layer into the bubble. The decrease of the bubble growth rate decreases the heat-transfer rate.

D. INTERNAL ENHANCEMENT

Internal enhancement increases the heat-transfer area, creates additional turbulence, and produces secondary flows, all of which contribute to the increase in the heat transfer. The laminar sublayer is assumed to be the principal resistance to heat transfer [Ref. 17: p. 6]. The developed secondary flow thins the sublayer and moves it into the stream where turbulence prevails and without an increase in shear; likewise, heat transfer is increased without an increase in friction [Ref. 18: p. 30]. Most studies show that the friction factor does increase with internal enhancement but the amount is strongly dependent on the internal enhancement geometry. The increase of both the friction and heat transfer is dependent on fin or rib pitch, groove depths, and helix angles [Refs. 17,19: pp. 6, 19-21]. Additionally, these studies have shown that there are

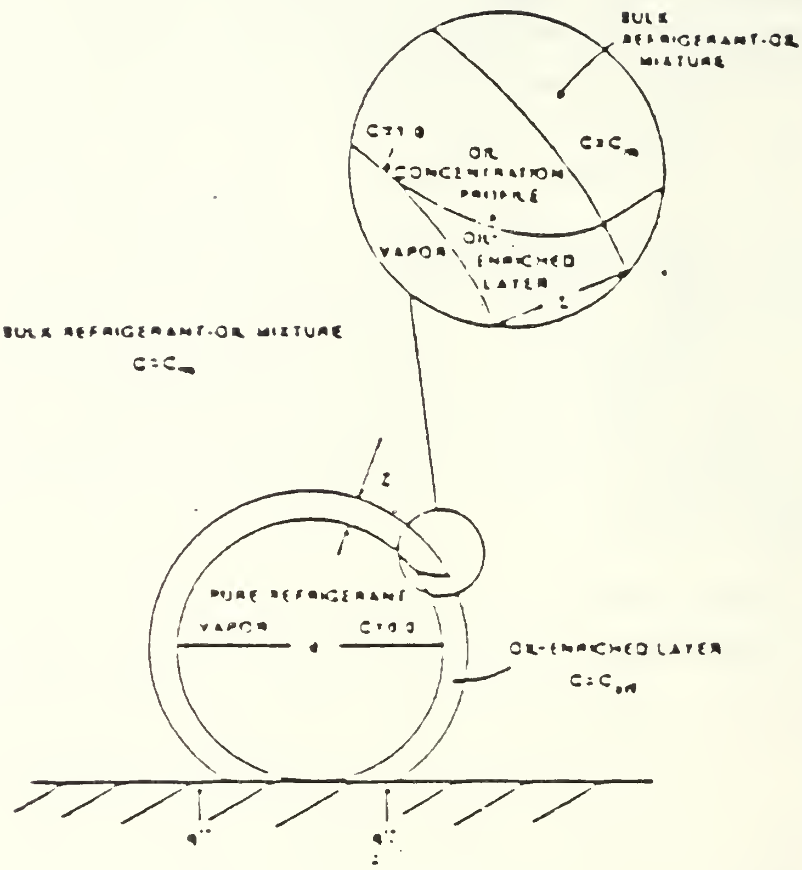

Figure 2.4. Idealized Model of Bubble Growth in Refrigerant-Oil Mixture (from Ref. 16).

critical geometrical dimensions that give the maximum heat transfer. For example, short fins (<< tube diameter) with rifling will raise heat-transfer coefficients with no problems of flow stagnation. Yet, medium fins may develop flow stagnation and decrease heat-transfer coefficients [Ref. 19: pp. 22-23]. As such, the selection of internal enhancement will generally improve the performance of boiling surfaces.

III. EXPERIMENTAL APPARATUS

A. OVERALL APPARATUS

A schematic of the experimental apparatus is given in Figure 3.1. The photographs in Figure 3.2 show two different views of the apparatus. Complete details on the design and construction of the refrigerant and oil components are given by Karasbun [Ref. 20: pp. 24-32]. A discussion of the modifications for the water heating mode is provided in this paper. The major components of the apparatus are: two Pyrex glass tees, an R-114 liquid reservoir, a water-ethylene glycol mixture sump, an R-12 refrigeration system, a vacuum pump, a water supply tank, three centrifugal pumps, a flow meter, three heaters, a graduated oil cylinder, and an oil reservoir. The R-114 boiling and condensation occurred in the lower and upper glass tees, respectively. The R-114 vapor was condensed by the water-ethylene glycol mixture pumped through a copper condenser coil located in the upper glass tee. A 1/2-Ton R-12 refrigeration system maintained the water-ethylene glycol mixture between -18 and -14 $^{\circ}$C.

The major difference between the experimental apparatus used by Karasabun and Reilly [Refs. 20,8: pp. 24-32, 30-35], and the one used during the present investigation concerned the use of water heating instead of electric heating as a means to provide heat to the boiling tube. Filtered tap water supplied from a storage tank (15), was pumped by two 1/2-hp motors (13 and 14) connected in series. A three-way valve (V-16) was provided on the downstream side of the second pump to obtain two flow paths. The normal flow path for data runs was through: the metering valve (V-17), the flowmeter (6), the inlet mixing chamber (16), the boiling tube, the outlet mixing chamber (16), the chambers provided

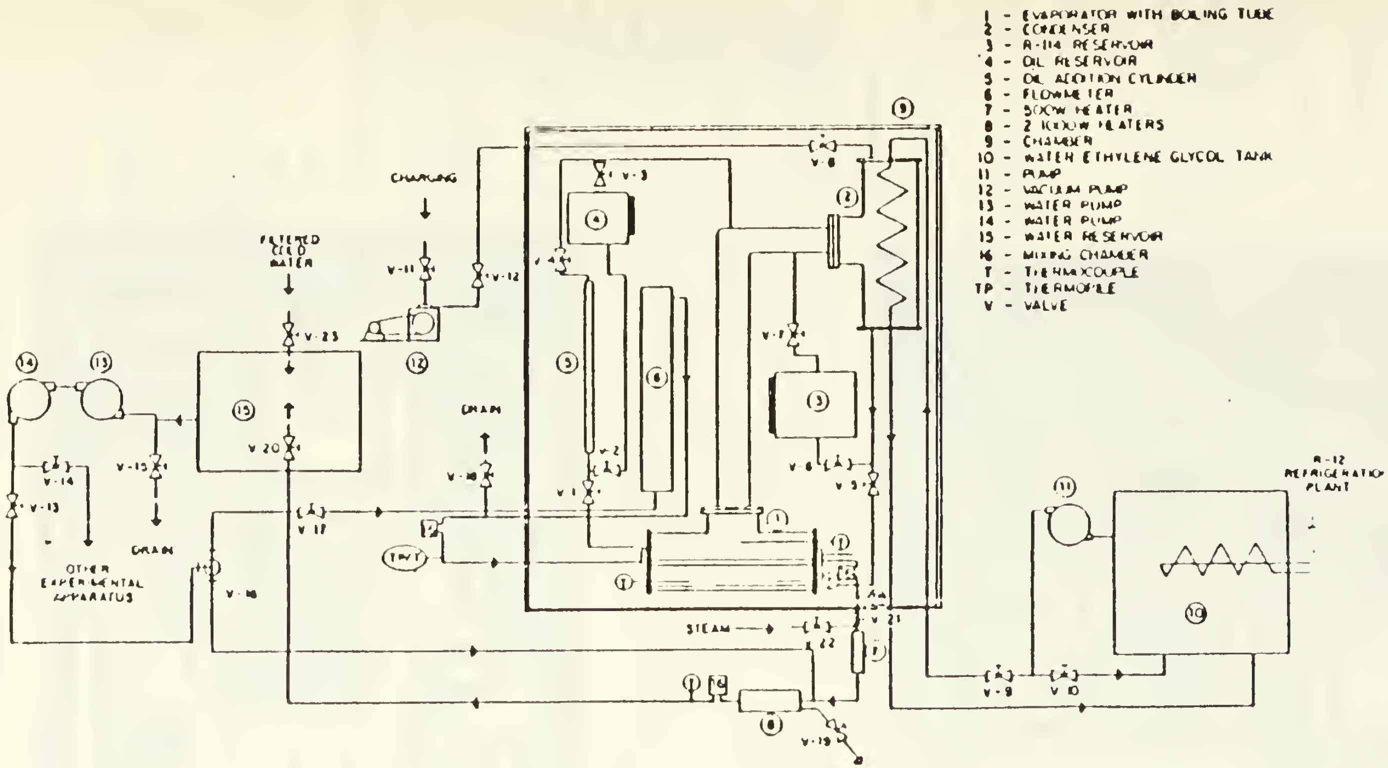

Figure 3.1. Schematic of Experimental Apparatus.

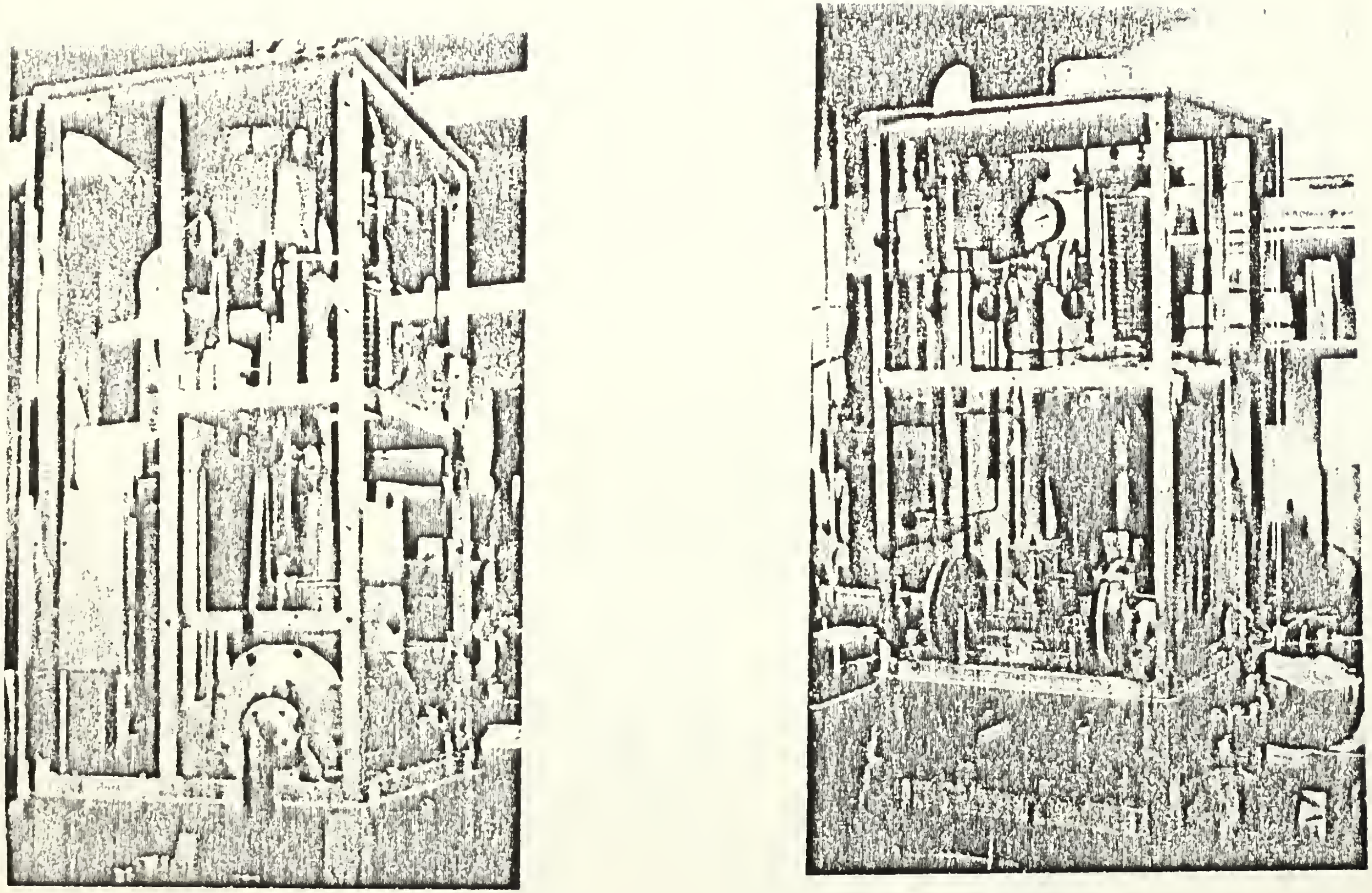

(a) (b)

Figure 3.2. Photographs of Experimental Apparatus: (a) Water Inlet Side, and (b) Front View.

with heaters (7 and 8), and returning to the storage tank through valve (V-20). The by-pass flow path was the same up to the three-way valve then the path was through heater chamber (8) and back to the storage tank through valve (V-20). Valves V-17 and V-21 were closed in order to isolate the boiling tube. This by-pass option was essential for preheating the water to higher temperatures, to achieve higher heat flux values in the boiling tube compared to values obtained from room-temperature water. A 500-W and two 1000-W heaters were used to maintain a steady water inlet temperature and to preheat the water. Flexible pressure hose was used for water piping throughout the apparatus. The mixing chambers and sections of hose connecting the mixing chambers to the boiling tube were double insulated to ensure accurate temperature measurements.

Copper-constantan thermocouples were used to measure thermal emf's for R-114 liquid and vapor, water inlet and outlet, and water-ethylene glycol mixture. A series-connected thermopile consisting of 10 junctions on either end was used to measure the temperature drop of the water from the inlet to the outlet of the boiling tube. This thermopile was calibrated against two quartz thermometer probes and agreement was found to be better than ± 0.02 K.

B. BOILING TUBE CONSTRUCTION

Figure 3.3 shows schematics of the smooth tube, and two enhanced tubes used. The tubes tested were:

1. a smooth copper tube;
2. a 90:10 copper-nickel corrugated tube (commercially referred to as Korodense tube) with an external, sintered porous coating (i.e. High Flux);
3. an internally and externally enhanced tube (alloy C12200) produced by Wolverine Division of U.O.P. (commerically referred to as Turbo-B);
4. a porous-coated (High Flux) Korodense tube with the porous coating machined off;
5. a Turbo-B tube with the external enhancement machined off.

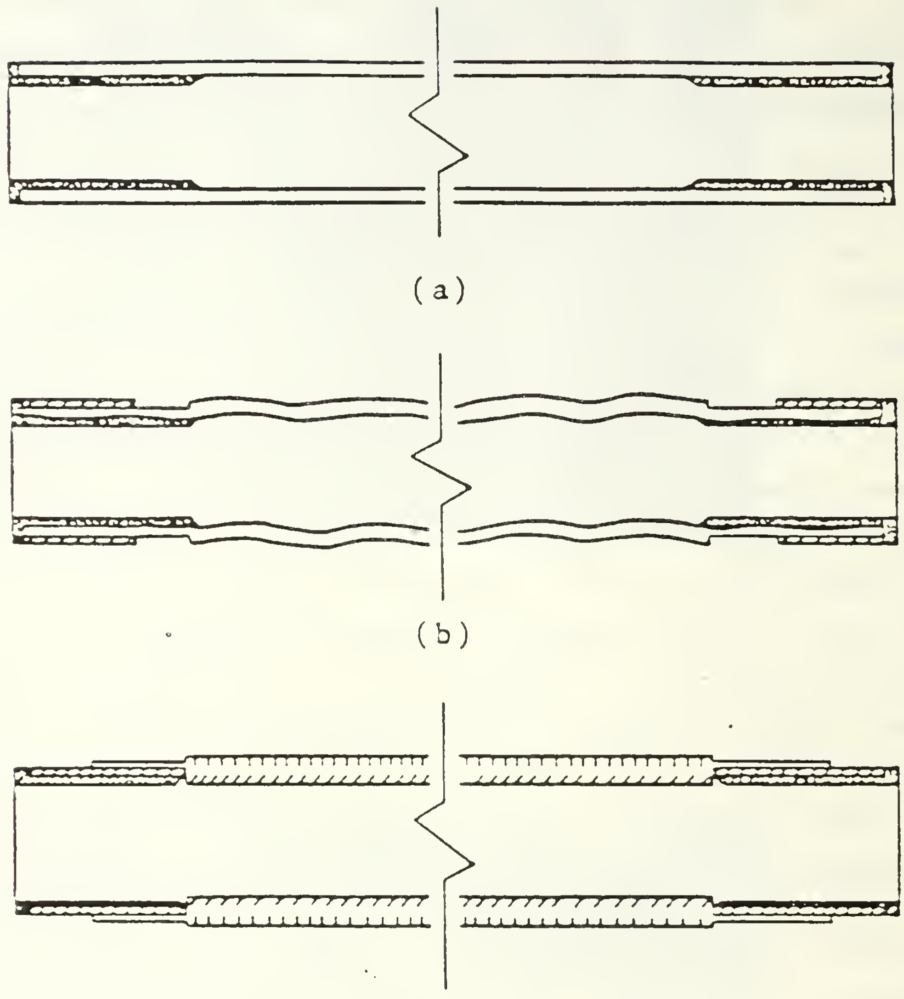

(a)

(b)

(c)

Figure 3.3. Schematic of Boiling Tubes: (a) Smooth Tube, (b) High Flux Coated Tube, and (c) Turbo-B Tube.

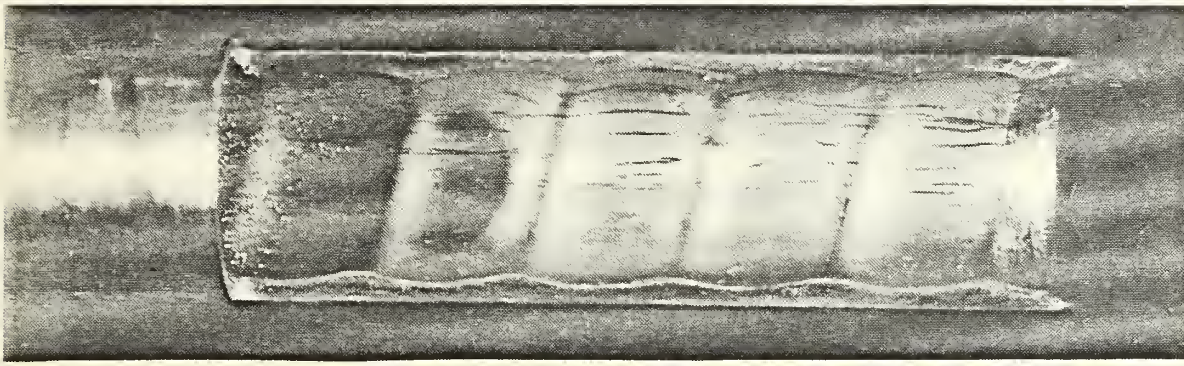

(a)

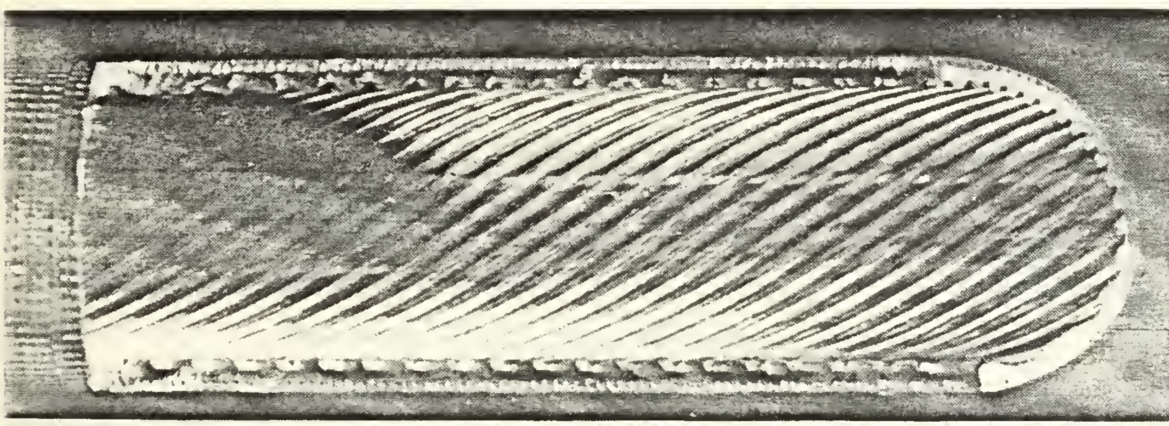

(b)

Figure 3.4. Photographs of Internal Enhancements: (a) Korodense Tube, and (b) Turbo-B Tube.

These tubes will be referred to as High Flux, Turbo-B, modified High Flux, and modified Turbo-B tubes, respectively, with the exception of tubes 2 and 4. Tubes 2 and 4 will be referred to as Korodense tubes with respect to discussions of only the internal enhancement. All of the tubes had an active (i.e., heated) section of 304.8 mm in length. The smooth, High Flux, and modified High Flux tubes had an outer diameter of 15.9 mm and an inside diameter of 12.7 mm. In the case of the High Flux tube, these diameters represent the values in the smooth portion of the tube (i.e., before performing the corrugation process). The Turbo-B tube had an external structured surface and a multiple-start helical ridged inner surface. This tube had an outer diameter of 16.9 mm at the base of the external structured surface and a minimum diameter of 14.5 mm at the internal ridge tips. The modified Turbo-B tube had identical diameters as the Turbo-B tube. The 63.5-mm-long inactive sections on either end was insulated by Teflon sleeves of 1.6 mm wall thickness located inside the boiling tubes, as shown in Figure 3.3. The requirement for using these two modified tubes is explained further in Chapter IV (EXPERIMENTAL PROCEDURES).

C. COMPUTER-CONTROLLED DATA ACQUISITION AND REDUCTION

Hewlett-Packard equipment was used for data acquisition, control, and analysis, as well as for storing of data. An HP-3497A acquisition unit was used to read the thermocouple and thermopile outputs. Table 1 gives the channel designations used.

Information entered by keyboard to an HP-9826A computer unit prompted and controlled the data acquisition unit. Data were analyzed and stored with the same computer unit. A step-by-step description of the data-reduction procedure is given in Appendix A, along with a printout of the program (DRP4) used.

TABLE 1

CHANNEL DESIGNATIONS

Channel	Function
0-1	R-114 liquid thermal emf's T(1) and T(2)
2	R-114 vapor thermal emf T(3)
3	water-ethylene glycol mixture thermal emf T(4)
4	water inlet thermal emf T(5)
5	water outlet thermal emf T(6)
20	thermal emf difference across water inlet and outlet T(7)

IV. EXPERIMENTAL PROCEDURES

A. FLOWMETER CALIBRATION

This section gives a brief description of the flowmeter calibration; a more detailed explaination is given in Appendix B. A Fischer Porter flowmeter was used to indicate percent water flow through the boiling tube. Prior to conducting any boiling runs, it was necessary to develop a correlation relating the flow percent to the mass flow rate and water velocity. Additionally, any temperature effect on viscosity would be incorporated into this correlation as a correction factor. Calibration runs were conducted over a temperature range of 19 °C to 38 °C and varying flowmeter settings. The correlation (equation (B.1)) was determined from these results. The correction factor for the viscosity temperature dependency was determined to be 1.0 with an accuracy of ± 0.02 as explained in Appendix B. In fact, it was not possible to find a systematic trend for this correction factor with the water inlet temperature. The stated accuracy mainly consists of the uncertainties involved with the visual reading of the flowmeter settings.

B. BOILING TUBE AND APPARATUS PREPARATION

The external surface of the boiling tube was cleaned with a Nitol (2% nitric acid and 98% ethyl alcohol) solution and both the external and internal surfaces were rinsed with acetone and were air dried prior to installation in the apparatus. A vacuum test at an absolute pressure of about 50 mm Hg was conducted on the refrigerant side of the apparatus after the boiling tube was installed. If no signs of leaks were evident after two hours, the system was pressurized to a gage pressure of about 250 mm Hg with R-114 vapor and the apparatus was checked for leaks with an automatic Halogen

Leak Detector. After fixing any leaks that may have been present, R-114 liquid was transferred from the reservoir to a pre-determined level in the boiling tee. This level gave a free surface 40 mm above the centerline of the boiling tube. At the set level, the mass of the R-114 liquid was computed to be 2.48 kg. A desired saturation temperature of 4 °C and the resultant system pressure were obtained by turning on the R-12 refrigeration system and varying the flow of cold (approximately -16 °C) water-ethylene glycol mixture through the condenser coil with valve V-9. At this saturation temperature and pressure, each boiling tube developed nucleation sites. The saturation temperature of 4 °C was maintained for at least 30 minutes prior to initiating nucleate boiling on the complete active length of the boiling tube.

The initiation of nucleate boiling could be done with cold water at 19 °C or with warm water at 25 °C through valve V-17 or with steam from a steam generation system through valve V-22. Early experimental data showed slight differences (up to 10 percent) in the computed outside heat-transfer coefficient depending on the highest heat flux at which the boiling was initiated on each boiling tube. As will be discussed in Chapter V (RESULTS AND DISCUSSION), the steam intiation method provided the highest initial wall superheat and ensured the best possible repeatability of the data. This intiation method was used for all of the runs unless otherwise specified.

Steam initiation was conducted by introducing steam through valve V-22 and discharging steam drain valve V-18 for about one minute. After this period, the three-way valve V-16 was shifted from a neutral position to the normal flow position. Valves V-22 and V-18 were closed and valve V-21 was opened simultaneously as the three-way valve was shifted to the normal position. Valve V-17 was opened wide prior to

shifting of the three-way valve. As these valves were shifted, warm water at 25 °C was pumped through the boiling tube at the maximum water velocity, which in turn gave the maximum heat flux for the given water inlet temperature.

C. BOILING DATA RUNS

Once the nucleate boiling initiation was completed, the saturation temperature was raised to 13.8 °C by adjusting valve V-9. This valve was also used to maintain this saturation temperature within ±0.05 K throughout a boiling run. The water inlet temperature was maintained to within ±0.08 K by using the heaters or introducing filtered cold water, respectively. The combination of heaters and cold water was used to maintain the desired water inlet temperature during each run. Two types of boiling runs were conducted at each oil mass percent.

The first type of run was conducted after holding the desired saturation temperature, water inlet temperature and initial flowmeter setting at steady-state conditions for about 10 minutes. After this period, the flowmeter setting was decreased with two data sets being taken at each flow setting. The two data sets were to show repeatability at each setting. The period between pairs of data sets was about 5 to 8 minutes, with steady state for each flowmeter setting maintained for at least 2 minutes. The second type of boiling run consisted of maintaining the previously mentioned initial steady-state conditions at a selected high water inlet temperature. The run was commenced by introducing cold water into the storage tank which lowered the water inlet temperature. While holding the water velocity constant, six to seven data points were taken, on a one time pass, at about every 0.3 K inlet temperature decrease. When the inlet temperature reached a selected low temperature, the steady-state conditions of the low inlet temperature,

water velocity, and saturation temperature of 13.8 °C were maintained for about 10 minutes. Then, the water inlet temperature was increased using the heaters, while holding the water velocity constant. Again, data points were taken on a one time pass, in about 0.3 K intervals, until the inlet temperature reached the previously used high inlet temperature.

Two complete boiling runs of the first type mentioned above were performed at 0% and 2% oil concentrations to further demonstrate repeatability. Table 2 shows the percent difference in wall superheat (i.e., ΔT) and heat flux for each boiling tube at these two oil percents. The higher percentages for the High Flux and Turbo-B tubes for the wall superheats are simply because of the low wall superheat values of these two tubes when compared to the values for the smooth tube. At these low superheat values, a small difference in the wall superheat leads to a larger percentage difference than that which occurs at higher wall superheats. The variation of the water inlet temperature was not considered a factor in this percent difference as the variation was less than ± 0.02 K per minute during these constant-inlet-temperature, decreasing-water-velocity runs.

TABLE 2

BOILING RUN REPEATABILITY

Tube	Oil%	ΔT	q
Smooth	0	± 9%	±20%
High Flux	0	±30%	±12%
Turbo-B	0	±30%	± 4%
Smooth	2	±10%	±25%
High Flux	2	±10%	± 2%
Turbo-B	2	±30%	± 2%

Note: initiations performed with steam

Additionally, data runs were conducted to determine the temperature increase across the boiling tube due to the pressure drop between the locations of the thermopile

probes. The data collected showed that this difference was less than the ±0.02 K accuracy of the thermopile and was considered negligible.

Following the boiling runs in pure R-114, oil was introduced to the boiling tee through valve V-1 from the graduated cylinder (5) shown in Figure 3.1. After the required volume of oil for a given oil mass percent was added, water at the maximum velocity was pumped through the boiling tube to promote vigorous boiling. This boiling ensured good mixing of the R-114 and oil mixture. Either another boiling run was conducted or the system was shut down to prepare for another steam initiation.

D. DATA ACQUISITION AND REDUCTION

The automatic data acquisition system was prompted to record the required thermal emf's, by keyboard inputs to the computer. The data were immediately processed and printed out on a hard-copy printer. A step-by-step procedure of data processing and reprocessing is given in Appendix A. Also, a printout of the data reduction program, DRP4, is included in this appendix. The heat flux, overall heat-transfer coefficient, outside boiling heat-transfer coefficient, and wall superheat values were computed based on the outside area expressed by the diameter if the enhancement of the outer surface was removed. Further, in order to account for the heat conduction through the inactive end sections, a correction was made for heat flux using an iterative computation procedure based on natural convection as discussed by Karasbun [Ref. 20: pp. 54-56].

When a boiling run was completed, the data were reprocessed by computer to obtain the inside and outside heat-transfer coefficients for further calculations. A Sieder-Tate-type constant (C_i) for the inside coefficient for each of the externally smooth tubes was calculated by using a modified Wilson plot [Ref. 22]. For the smooth tube,

modified High Flux, and modified Turbo-B tubes, the outside coefficient was calculated simultaneously using the correlation (equation: (C.3) and (C.4)) developed by Rohsenow [Ref. 23: p. 969], and the modified Wilson plot. The Rohsenow correlation is based on externally smooth tubes, thus the requirement for the modified High Flux and Turbo-B tubes. A further explaination of the modified Wilson plot is given in Appendix C. The C_i values found for the externally smooth tubes were used for the corresponding externally enhanced tubes. Knowing the inside coefficient, the outside coefficient for the boiling tubes were computed by subtracting the inside and wall resistances from the measured overall thermal resistance (equation: (C.7)).

V. RESULTS AND DISCUSSION

A. INSIDE HEAT-TRANSFER COEFFICIENT

Results were obtained for the smooth, High Flux, and Turbo-B boiling tubes at a boiling temperature of 13.8 °C and at oil concentrations of 0, 1, 2, and 6 mass percent. The heat flux versus wall superheat for these three tubes is shown in Figure 5.1. All three tubes are in the nucleate boiling range with decreasing heat flux. It can be seen that the High Flux and Turbo-B tubes outperform the smooth tube throughout the tested heat flux range. Additionally, the Rohsenow correlation for a smooth tube at a boiling temperature of 13.8 °C with the experimentally determined (from the modified Wilson plot) C_{sf} coefficient of 0.0060 is shown in this figure.

The Rohsenow correlation, as used in the modified Wilson plot, has an exponent of r = 1/3. Yet, this correlation is very sensitive to the r value. A change in this exponent of three percent yielded a change in the C_{sf} only of 0.016 percent but gave a change of 17 percent in the Sieder-Tate-type constant inferred from the modified Wilson plot. For the purpose of data analysis, the value or r = 1/3 was used, while knowing that an additional uncertainty was being introduced by this exponent.

For each externally smooth tube, the Sieder-Tate-type constant was computed using the modified Wilson plot based on 5 to 10 different runs in pure R-114. The computed values for the smooth, Korodense, and Turbo-B tubes were 0.036 ±0.002, 0.066 ± 0.005, and 0.077 ± 0.003, respectively. For the smooth tube, the experimentally found Sieder-Tate-type constant is 33 percent greater known than the well-known value of 0.027 for long internally smooth tubes with fully developed flow. This larger constant

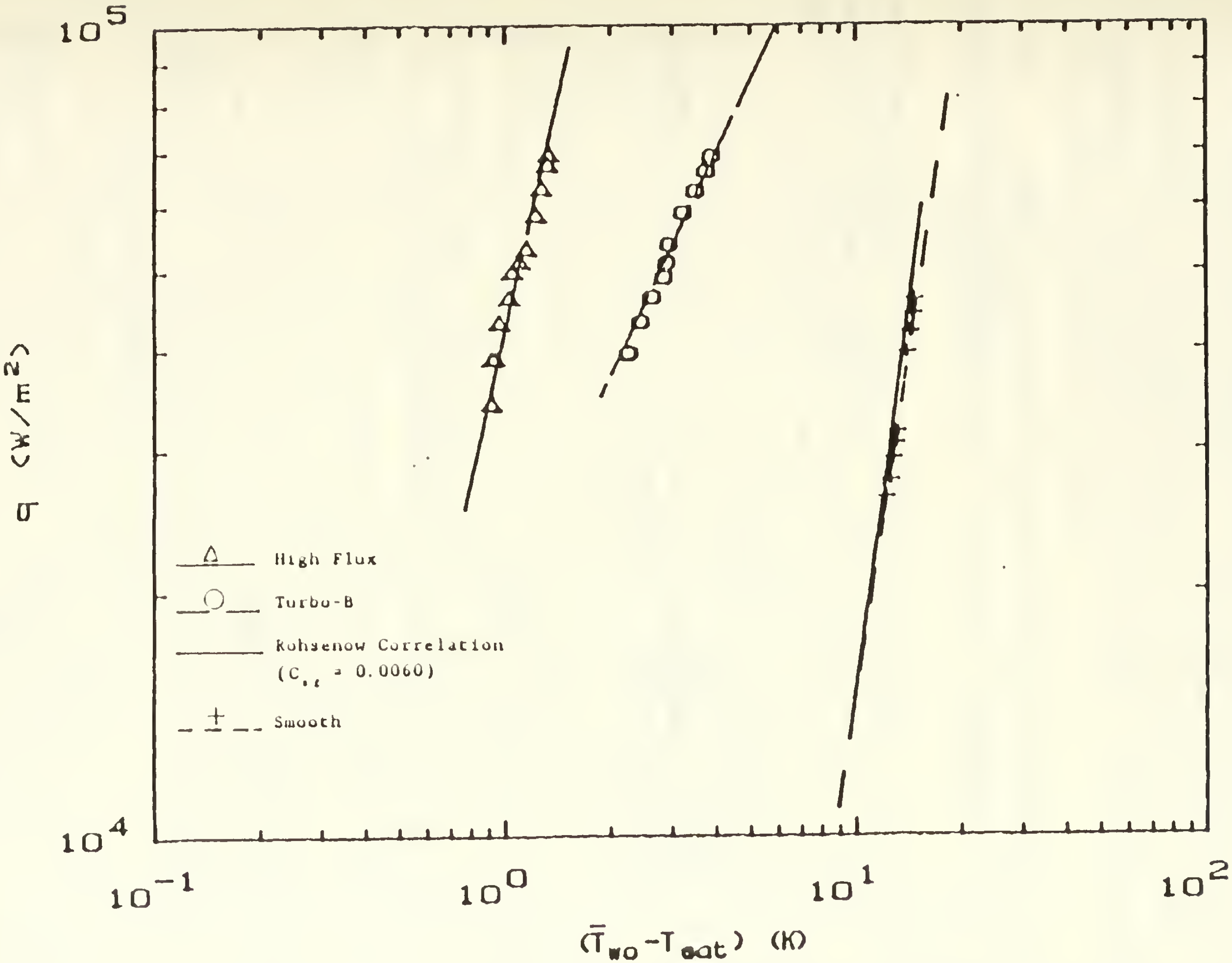

Figure 5.1. Variation of Heat Flux with Wall Superheat at 0% Oil.

appears to be the result of the entrance effects of the shorter experimental tube and the uncertainty introduced by the exponent r of the Rohsenow correlation as discussed above. The minimum entrance length for a fully developed pipe flow is given, as a rule of thumb, by Incropera and DeWitt [Ref. 24: p. 406] as

$$\frac{L_e}{D} = 60 \tag{5.1}$$

for Reynolds numbers greater than or equal to 10000. Also, as the pipe roughness increases the minimum entrance length decreases.

Withers has developed Stanton number correlations for tubes with single-helix and multiple helix ridging [Refs. 25,26: pp. 52-56,44]. These correlations are listed below. For single-helix ridging,

$$St = \frac{\sqrt{\frac{f}{8}}\,Pr^{-0.5}\left(\frac{p}{d_i}\right)^{0.33}}{7.22\left[\left(\frac{e}{d_i}\right) Re\left(\frac{f}{8}\right)^{0.5}\right]^{0.127} + \gamma} \tag{5.2}$$

$$\sqrt{\frac{f}{8}} = -\frac{1}{2.46\,\ln\left[r + \left(\frac{7}{Re}\right)^{m}\right]} \tag{5.3}$$

where r and m are determined by tube dimensions, and

$$\gamma = -\left\{2.5\,\ln\left[2\left(\frac{e}{d_i}\right) + 3.75\right]\right\} \tag{5.4}$$

For multiple-helix ridging,

$$St = \sqrt{\frac{f}{8}}\,Pr^{-0.5}\left[\frac{1}{8^{\#}\left(Re\sqrt{\frac{f}{8}}\right)^{0.136} + \gamma}\right] \tag{5.5}$$

$$\sqrt{\frac{f}{8}} = -\frac{1}{2.46\,\ln\left[r + \left(\frac{\;}{Re}\right)^{m}\right]} \tag{5.6}$$

r and m again are functions of tube dimensions,

$$\gamma = -\left\{2.5\ln\left[2\left(\frac{e}{d_i}\right) + 3.75\right]\right\} \tag{5.7}$$

and

$$B^{\#} = 5.68\left(\frac{e}{p}\right)^{-\frac{1}{8}}\left(\frac{e}{d_i}\right)^{0.136} \tag{5.8}$$

A comparison of Stanton numbers was made for the modified Korodense and modified Turbo-B tubes using the following equations for these two tubes:

$$St = \frac{h_i\ D_i}{k_f\ Re\ Pr} \tag{5.9}$$

where

$$h_i = C_i\ \frac{k}{D_i}\ Re^{0.8}\ Pr^{0.33}\left(\frac{\mu}{\mu_w}\right)^{0.14} \tag{5.10}$$

The results for these two modified tubes were compared to a copper Korodense (i.e., single-helix ridging) and a Turbo-Chill (i.e., multiple-helix ridging) tubes, respectively. The latter two tubes tested by Withers were similar in radial dimensions but were 1.5 meter long. The predicted St numbers using equations (5.1) - (5.8) for the Withers' Korodense and Turbo-Chill tubes were 0.00177 and 0.00273, respectively. The experimental St numbers using equations (5.9) and (5.10) for the modified Korodense and modified Turbo-B tubes were 0.00242 and 0.00286, respectively. The majority of the difference between the predicted and experimental St numbers may be attributable to the entrance effects and the uncertainity introduced by the Rohsenow correlation.

B. LIGHT OFF EFFECTS

As referred to in Chapter IV, Figure 5.2 shows the light off effects for the smooth, High Flux (i.e., porous-coated Korodense), and Turbo-B tubes. These effects are most probably due to the requirement of greater heat flux to initiate

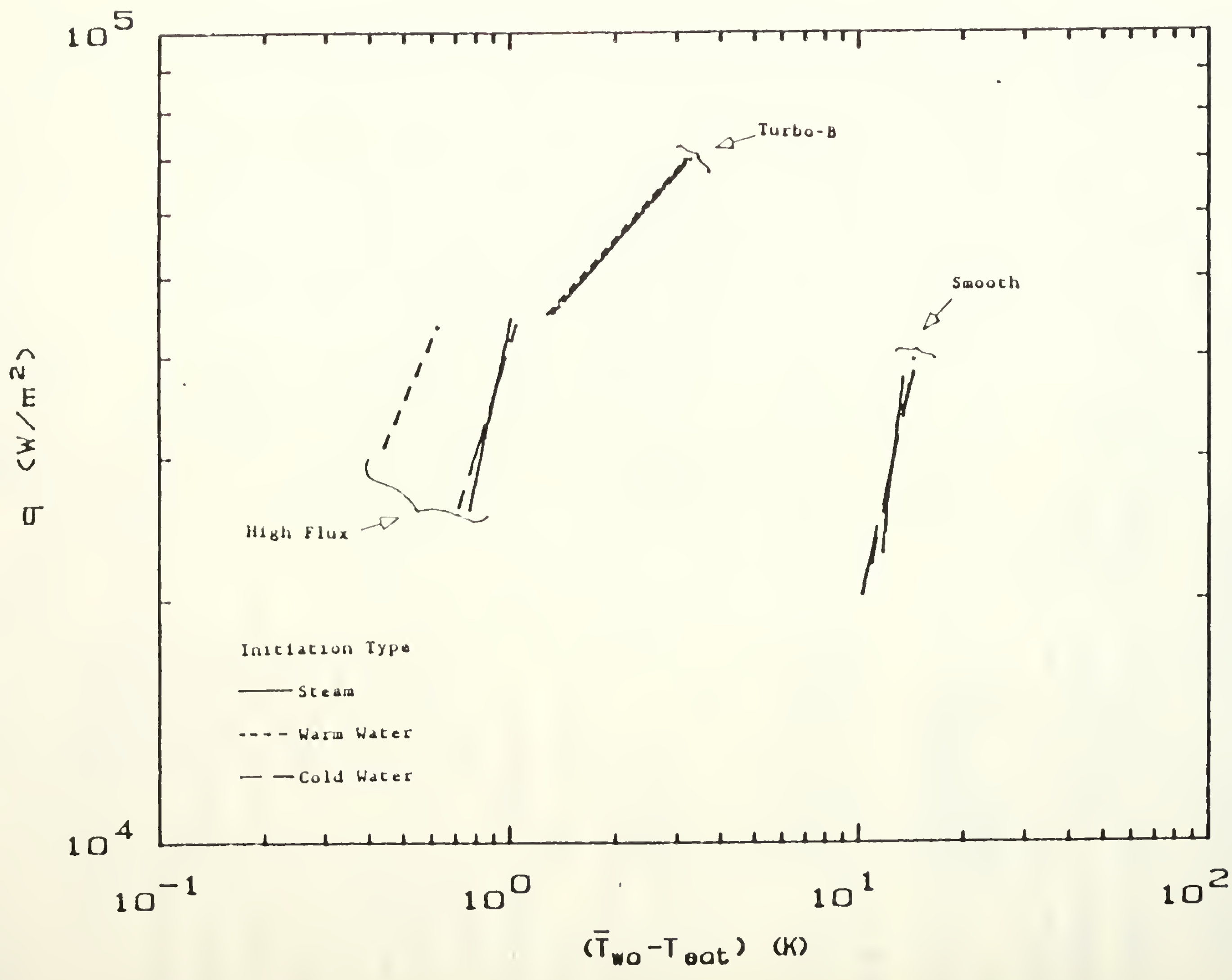

Figure 5.2. Light Off Effects at 0% Oil.

the nucleation sites than the heat flux required to maintain the sites once they are activated. As the boiling tube sits in the R-114 liquid, prior to initiation, reentrant cavities or the nucleation sites flood with liquid. The initial formation of the vapor bubbles and thus the initiation of the nucleation site requires the input of a greater heat flux or higher wall superheat. Figure 5.3 shows the boiling tube initiation with steam for the smooth, High Flux, and Turbo-B tubes [Refs. 21,7: p. 478, 62]. As shown in Figure 5.3, the High Flux tube is more sensitive to light off effects. This sensitivity is mostly due to the lower wall superheats at which nucleation occurs. A change of .5 of a degree is more pronounced at these lower wall superheats than a similar change at the wall superheats for the Turbo-B and smooth tubes.

C. SMOOTH TUBE

Figure 5.4 shows the performance of the smooth tube at 0, 1, 2, and 6 mass percent oil concentration at 13.8 °C. Reilly's [Ref. 8: p. 65] data for the electrically heated smooth tube at a boiling temperature of -2.2 °C in pure R-114 liquid are also included for comparison. The differences between the experimental results shown and Reilly's data are probably due to physical characteristics introduced in the electrically heated tube when soldering the copper sleeves (inside of which the electric heaters were fitted) on the interior of the tube. As discussed by Reilly [Ref. 8: pp. 57-61], the contact resistance at the interface between the sleeve and the inner surface of the tube was minimized by tinning. However, the tinning process may not have been 100 percent successful, thereby introducing unacceptable uncertainties into the experimental measurements. Further Reilly reported considerable variations (up to 3 K at a heat flux of 98 kW/m^2) in the measured wall temperatures. Reilly attributed this observation to an axially non-uniform heat flux generated by the cartridge heater.

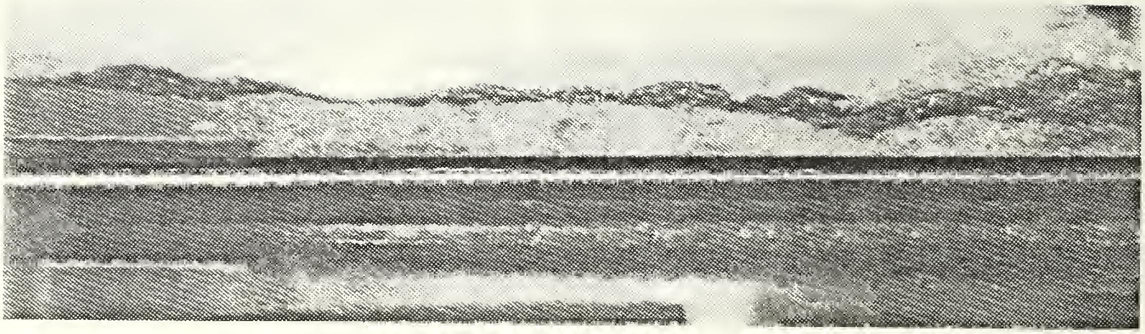

(a)

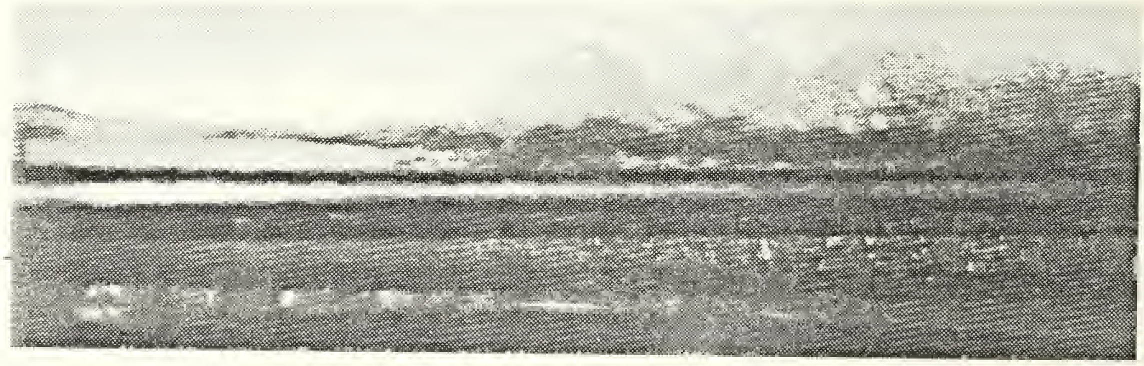

(b)

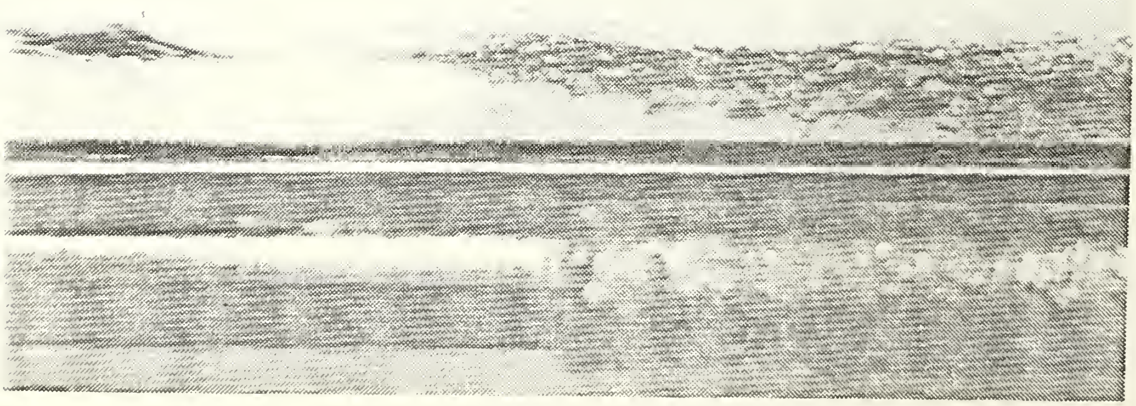

(c)

Figure 5.3. Photographs of Steam Initiation: (a) Smooth Tube (b) High Flux Tube, and (c) Turbo-B Tube. Note: Bar in front of boiling tubes is an auxilliary heater.

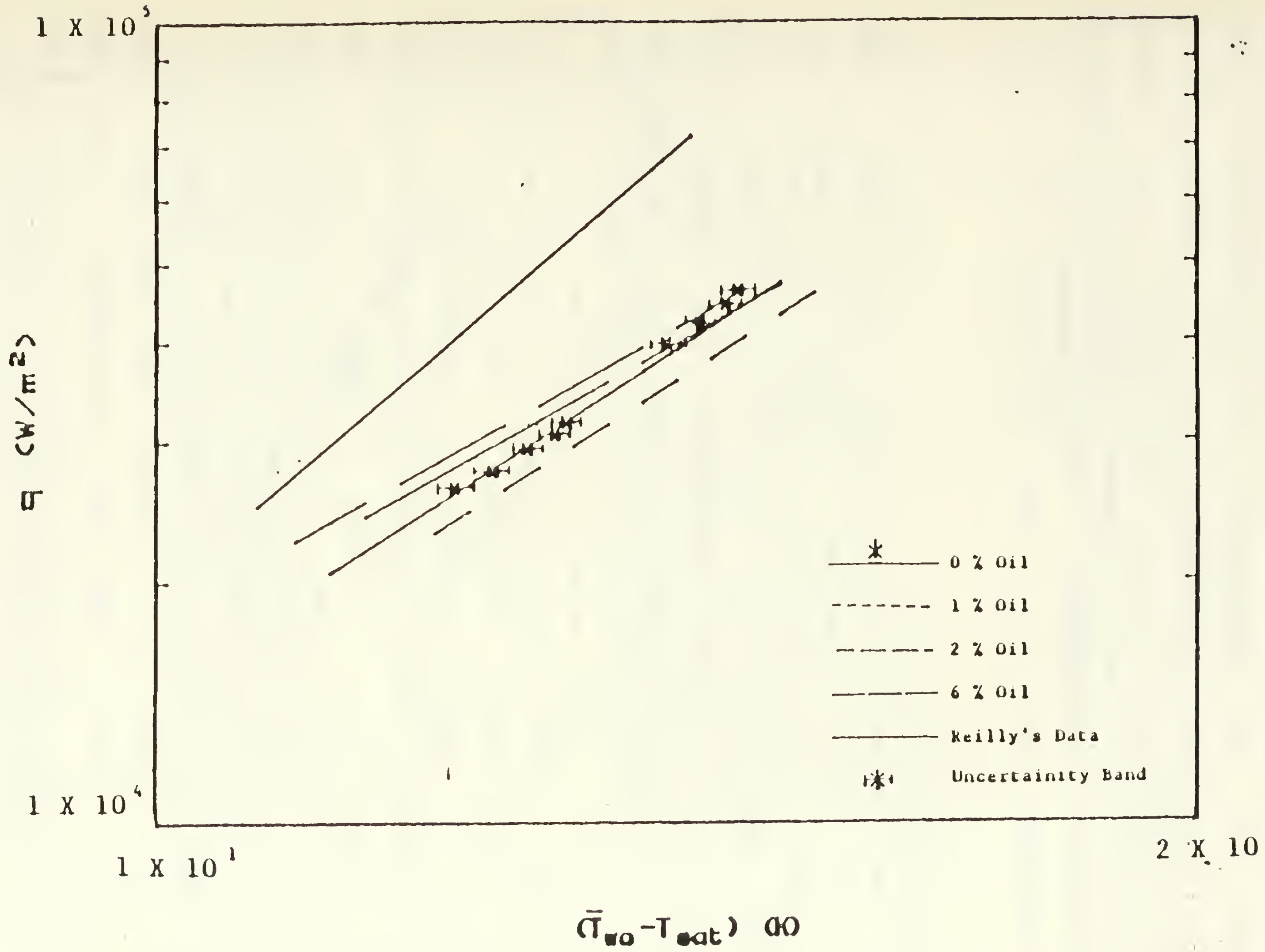

Figure 5.4. Variation of Heat Flux with Wall Superheat for Smooth Tube.

As shown in Figure 5.4, the wall superheat increased for 1 percent oil concentration and decreased slightly for 2 and 6 percent oil. This decrease in the wall superheat for the higher oil percentage is possibly due to the enhanced bubble formation experienced by the tube because of the foaming action of the R-114 and oil mixture decreasing resistance to heat transfer as explained by Chongrungreong [Ref. 5: p. 701], Nobukatsu [Ref. 27: p. 60], and Chaddock [Ref. 21: p. 474].

D. HIGH FLUX TUBE

The performance of the High Flux tube in terms of heat flux versus wall superheat is given in Figure 5.5. Additionally, this figure shows Reilly's data [Ref. 8: p. 70], for the electrically heated High Flux tube in pure R-114 at a 6.7 °C boiling temperature. The presence of oil increased the wall superheat, at a heat flux of 40 kW/m^2, by a factor of 1.22 for 1 percent oil and a factor of 2.12 for 6 percent oil. The number of nucleation sites reduced considerably and the foaming action increased significantly as the oil mass percent increased. These actions are shown in Figure 5.6. With 6 percent oil concentration, it was visually observed that the nucleation sites were active only in the corrugations, as shown in Figure 5.6 (c). This congregation of sites is due, in part, to the sparser porous coating on the high points of the tube and the decreased wall thickness in the corrugations. As a result of the corrugation process during tube manufacture, the wall thickness at the corrugation is smaller than the rest of the tube, which implies lower wall resistance. During the sintering process, the coating appears to have concentrated in these corrugations giving a thicker coating of copper particles and increased number of nucleation sites compared to the rest of the tube surface.

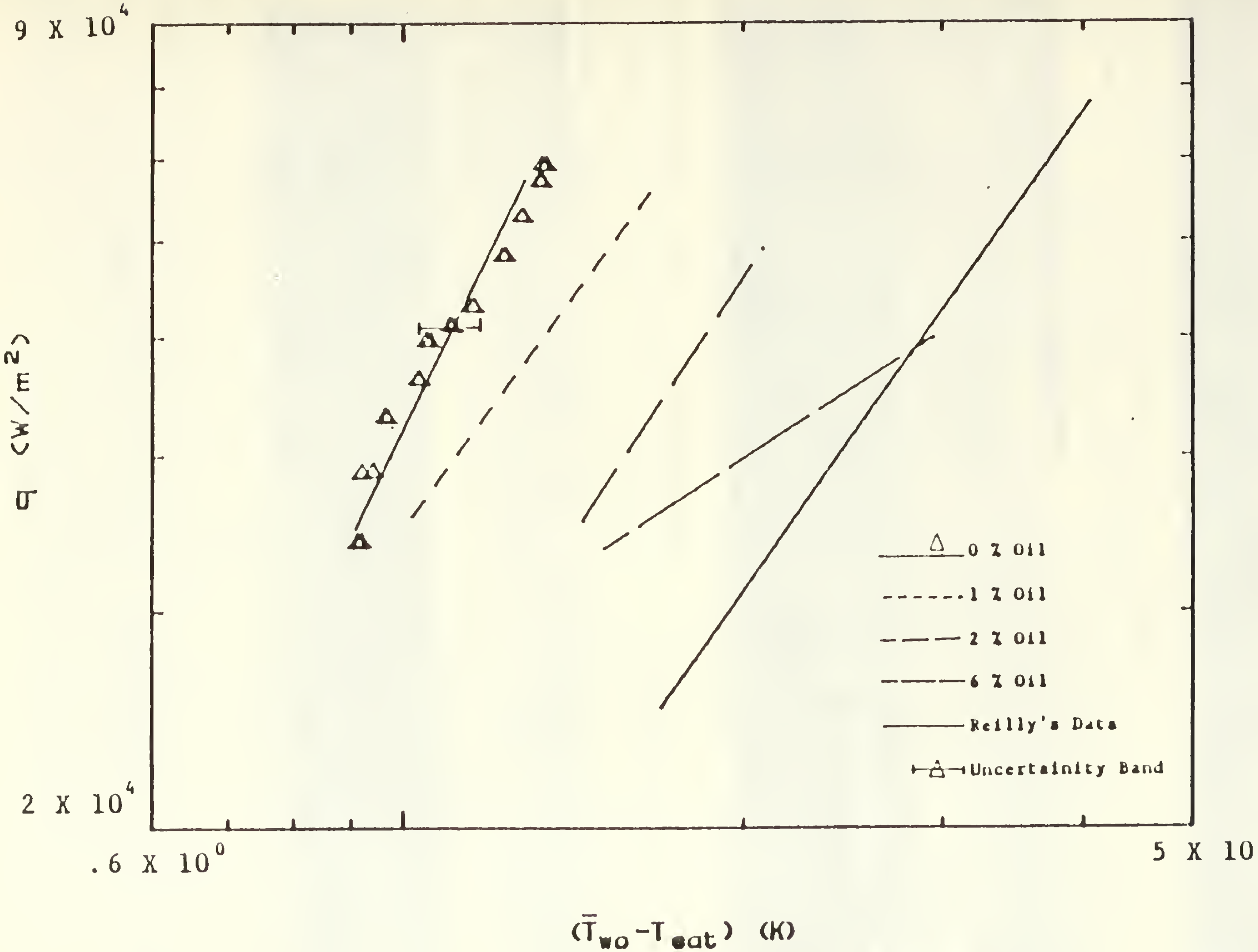

Figure 5.5. Variation of Heat Flux with Wall Superheat for High Flux Coated Tube.

(a)

(b)

(c)

Figure 5.6. Photographs of Boiling from High Flux Coated Tube: (a) 0%, (b) 2%, and (c) 6%. Note: Bar in front of boiling tube is an auxillary heater

The increase of the wall superheat, when oil is present, is possibly the result of increased surface tension and viscosity. The increasing surface tension and viscosity lead to the formation of an oil-rich layer next to the boiling surface. This oil-rich layer has an insulating and inhibiting of bubble growth effect within the cavities. The higher liquid-vapor surface tension and surface tension in the oil-rich layer requires more energy for the formation and growth of the bubble. Additionally, diffusion processes affect the bubble formation. Oil concentrations near the boiling surface are high compared to the concentration in the bulk liquid and diffusion occurs from the cavity into the bulk liquid. This diffusion continues until an equilibrium point is reached. If oil-rich layers are developing on the boiling surfaces, the diffusion from the cavities to the bulk liquid slows down aiding the further build-up of the oil-rich layer. The vapor bubble forming in the cavity also has an oil vapor content which is undergoing its own diffusion process. As the refrigerant evaporates through the oil-rich layer into the interior of the bubble, it must overcome large diffusion resistances set up by the oil vapor within the bubble. The increased surface tension, viscosity, diffusion resistance and the decreasing bubble formation rate contribute to the decrease in the heat-transfer coefficient and the increase in the wall superheat at a given heat flux. [Refs. 5,21,28,29,30: p. 702, 477-478,59,372,82]

Also, boiling runs were conducted holding the water velocity constant and allowing the water inlet temperature to decrease and then to increase. The decreasing and increasing heat flux with the respective change in the water inlet temperature versus wall superheat is shown in Figure 5.7. The motion of the hysteresis (i.e., clockwise or counterclockwise) depended on the temperature starting point. If the temperature was decreased and then increased, the motion

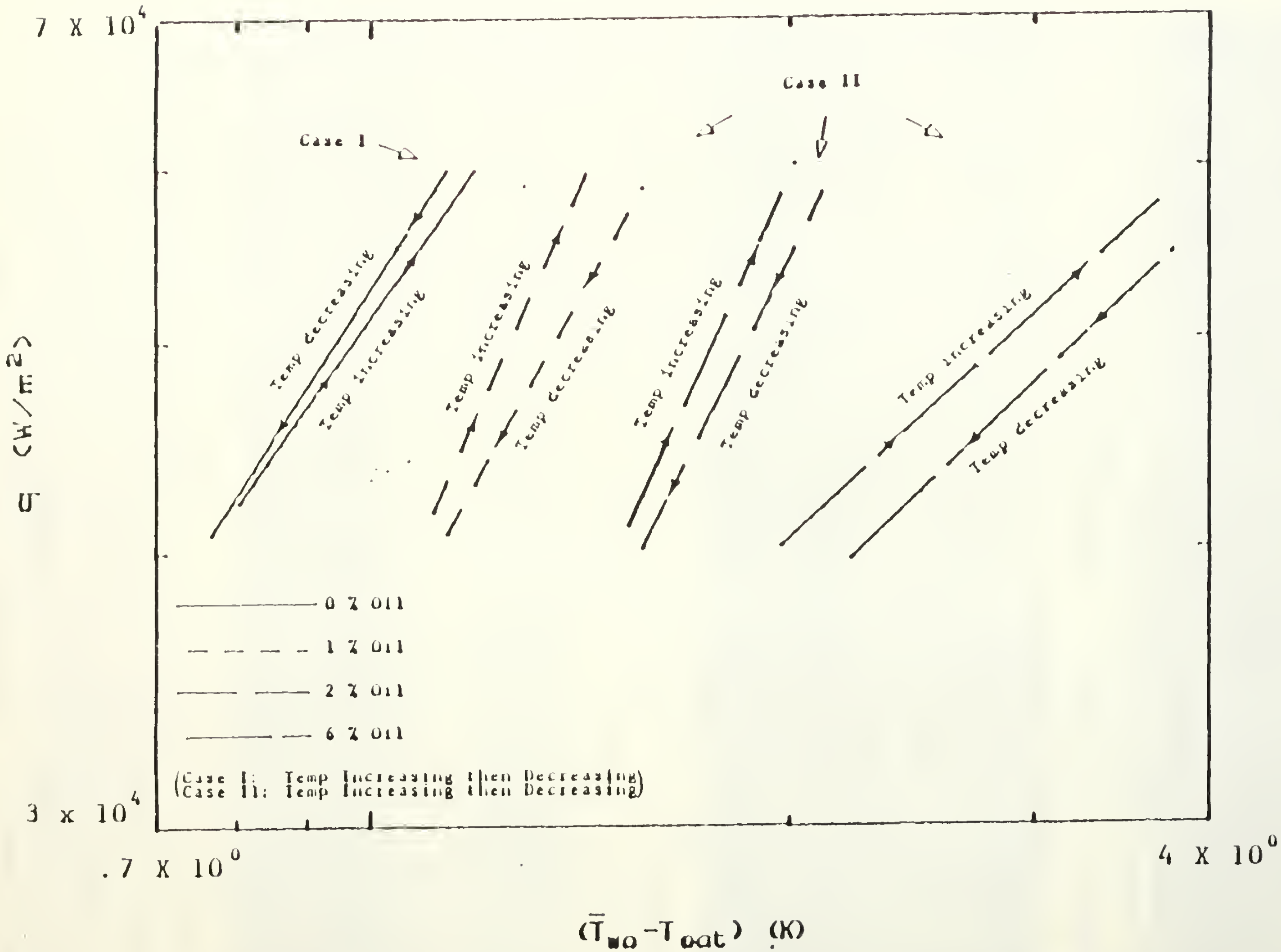

Figure 5.7. Variation of Heat Flux with Changing Water Inlet Temperature for High Flux Coated Tube.

was clockwise. When the temperature was increased and then decreased, the motion was counterclockwise. This directional change is related to the amount of heat flux required to maintain active nucleation sites. In the first case of temperature decreasing then increasing, less heat flux is needed to maintain the same amount of sites, but, at the same time, heat flux decrease as the water heat capacaity is decreasing. In the second case, with the water inlet temperature increasing then decreasing, the water heat capacity increases so the heat flux increases raising the wall superheat and the heat-transfer coefficient.

E. TURBO-B TUBE

Figure 5.8 shows a similar relationship as Figure 5.5 but for the Turbo-B tube. The increase in wall superheat, for a heat flux of 40 kW/m^2, ranges from a factor of 1.04 for 1 percent oil to a factor of 1.37 for 6 percent oil. The Turbo-B tube remained active over the full active length of the tube, as shown in Figure 5.9. The apparent decrease of nucleation sites, as shown by the High Flux tube, did not occur with the Turbo-B tube. As discussed pertaining to the High Flux tube, the increase in the wall superheat with increasing oil concentration is probably due to the increased surface tension and viscosity of the mixture within the cavities. Also, Boiling runs for constant water velocity and varying water temperature were performed on the Turbo-B tube and are also shown in Figure 5.10. The same hysteresis motions observed with the High Flux tube are observed with the Turbo-B tube.

F. COMPARISON OF BOILING HEAT-TRANSFER COEFFICIENTS

The ratios shown in Figure 5.11 are h/h for the Turbo-B and High Flux tubes and h/h_s for the smooth tube. All of the ratios were taken at a heat flux of 40 kW/m^2. The High Flux tube shows the most significant effect due to oil

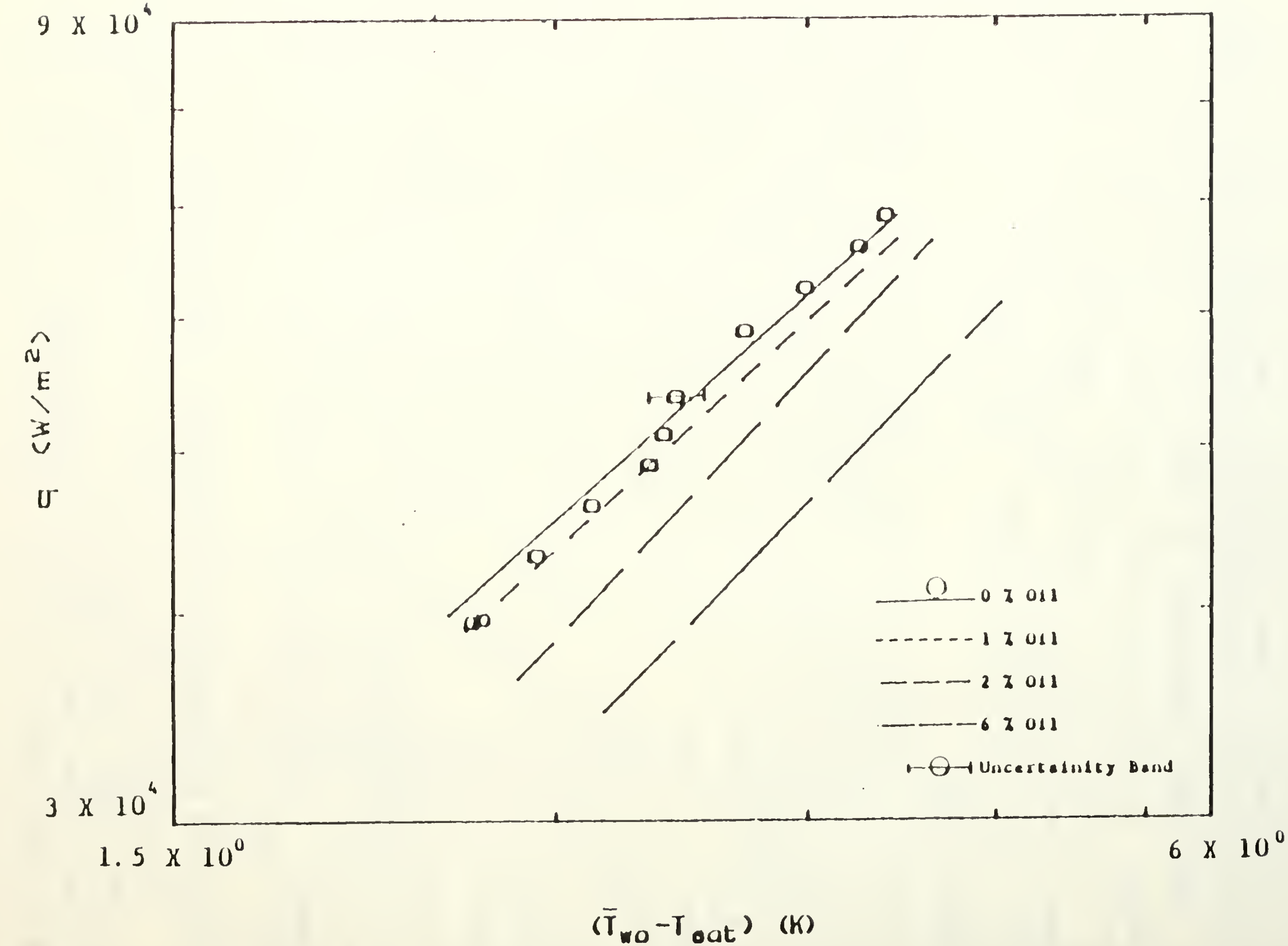

Figure 5.8. Variation of Heat Flux with Wall Superheat for Turbo-B Tube.

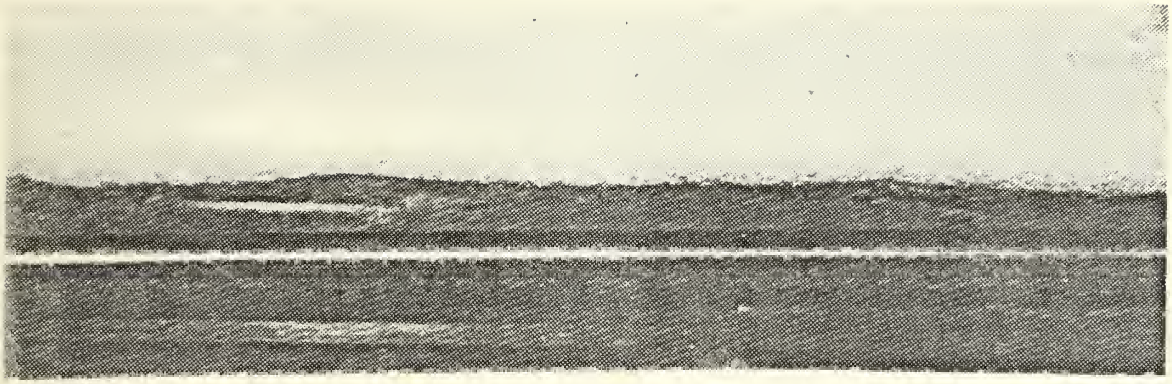

(a)

(b)

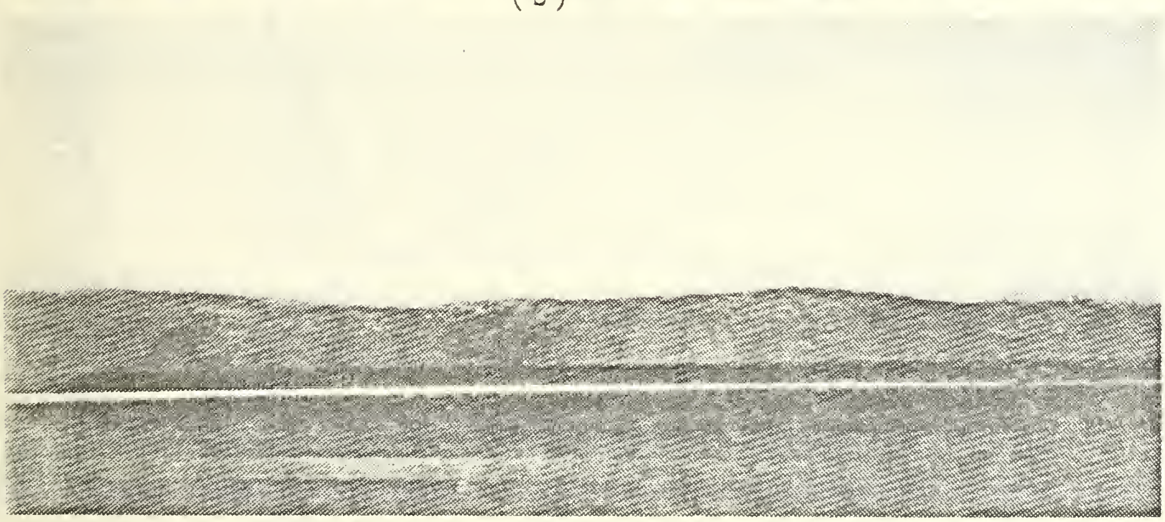

(c)

Figure 5.9. Photographs of Boiling from Turbo-B Surface: (a) 0%, (b) 2%, and (c) 6% Oil Mass Percents.
Note: Bar in front of boiling tube is an auxillary heater.

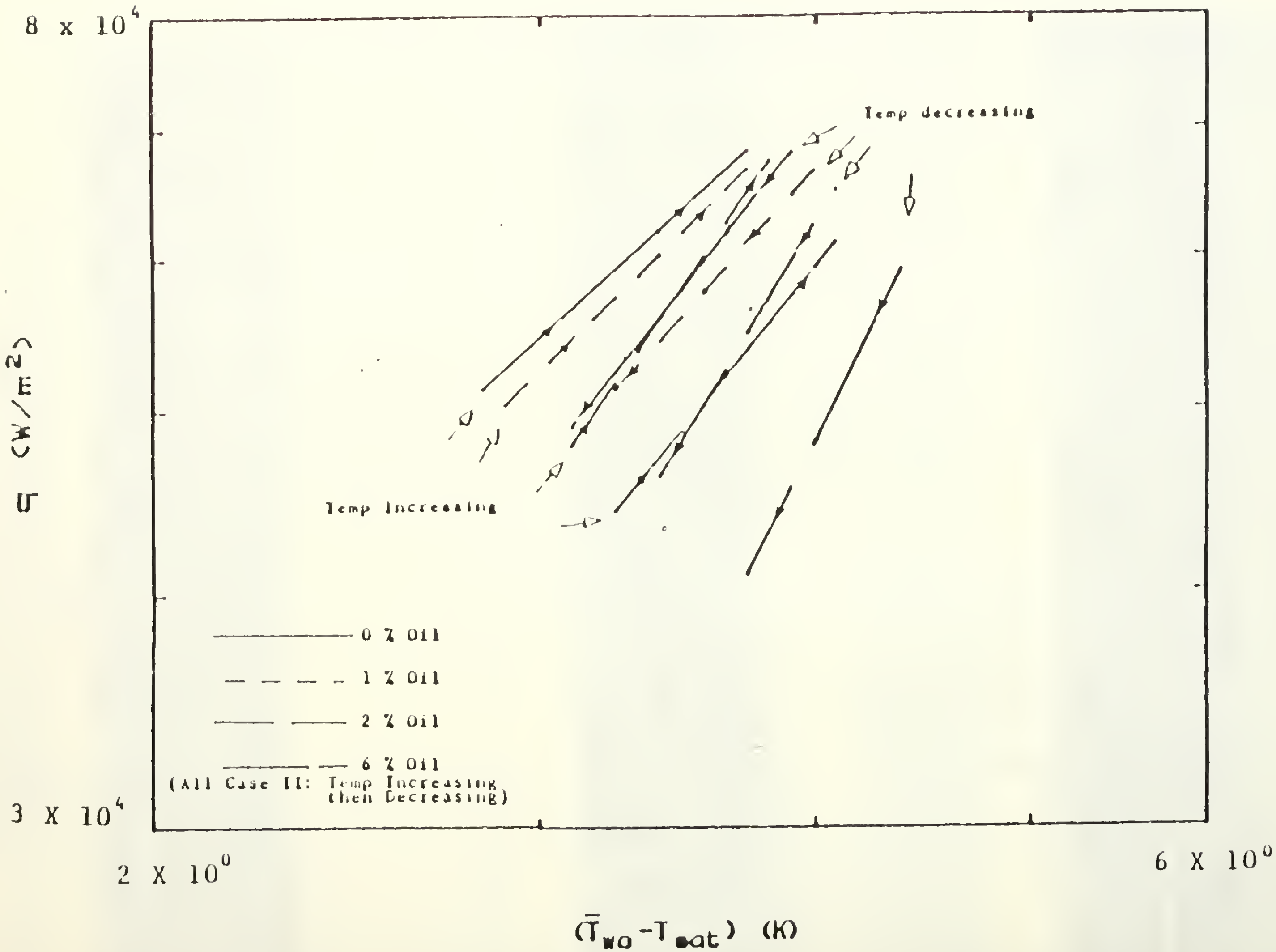

Figure 5.10. Variation of Heat Flux with Changing Water Inlet Temperature for Turbo-B Tube.

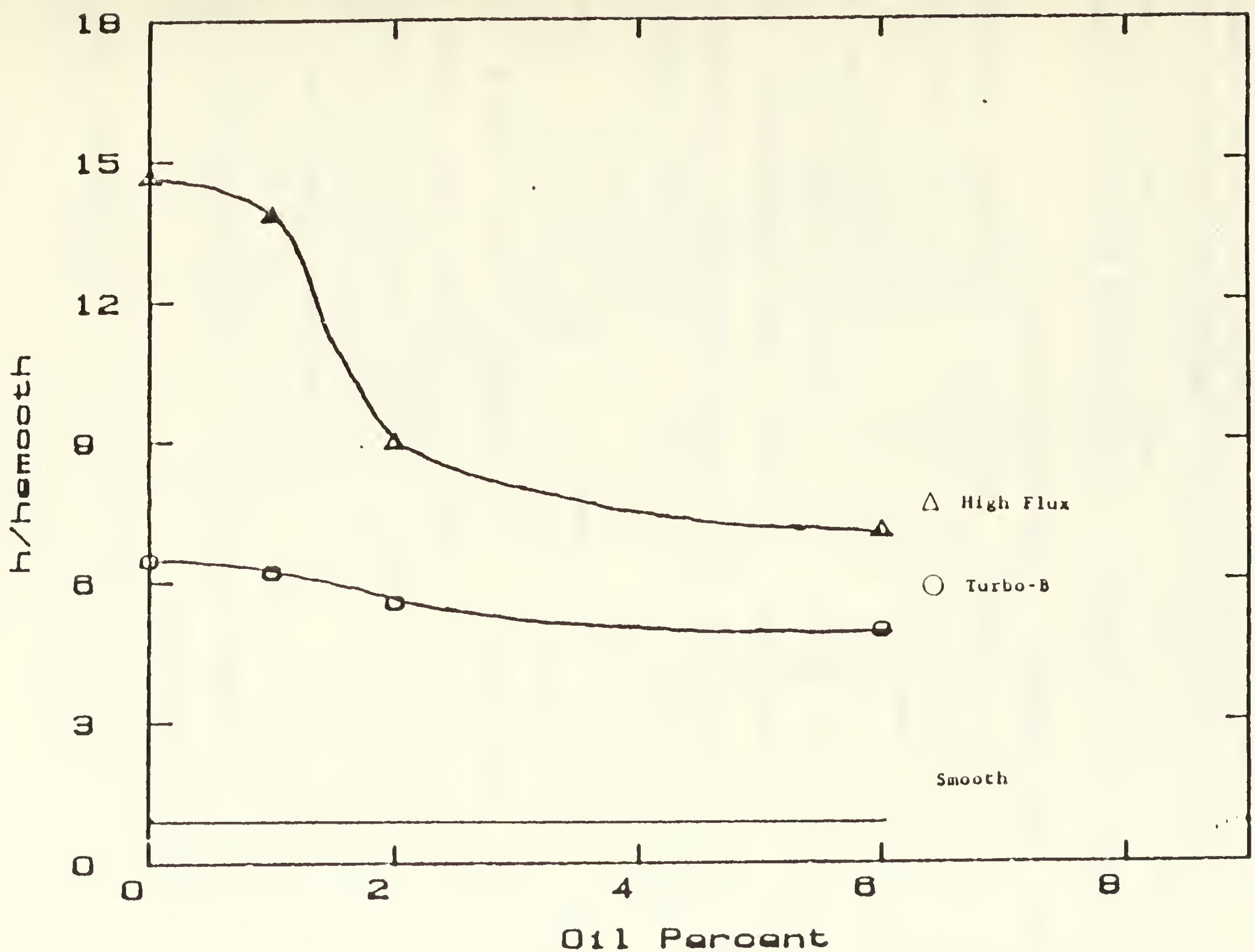

Figure 5.11. Variation of Boiling Heat-Transfer Ratio with Oil Mass Percent for a Heat Flux of 40 kW/m^2.

concentration which is due to the reasons previously discussed. The h/h_s ratio for the High Flux tube decreased by 65 percent. For the Turbo-B tube the rate of degradation of the boiling heat-transfer coefficient is less pronounced. The Turbo-B tube shows a decrease of 24 percent at 6 mass percent oil. The larger cavity size of the Turbo-B tube, compared to the High Flux tube, results in smaller oil concentrations in the oil rich layer. This observation may explain the smaller degradation experienced by Turbo-B tube.

G. OVERALL HEAT-TRANSFER CHARACTERISTICS

The overall heat-transfer coefficient versus decreasing water velocity for oil mass percents of 0, 2, and 6 for each boiling tube is shown in Figure 5.12. For pure R-114 with a water velocity of 2 m/s, the Turbo-B tube outperforms the High Flux tube by a factor of 1.13 and the smooth tube by a factor of 4. While the High Flux tube outperformed the Turbo-B tube based on the outside heat-transfer coefficient, the reverse is true for the overall heat-transfer coefficient. This relationship in U_o is due in part to the increased internal enhancement of the Turbo-B tube. Comparison of the Sieder-Tate-type constants for the Turbo-B and High Flux tubes (see p. 34) shows that the Turbo-B tube has a 17 percent greater inside coefficient than the High Flux tube. Both of the enhanced tubes dramatically outperformed the smooth tube. It should be noted that the increase in pressure drop due to internal enhancement (compared to a smooth-interior case) was not considered here. The pressure drop would be an important factor in finally selecting the most economical tube type.

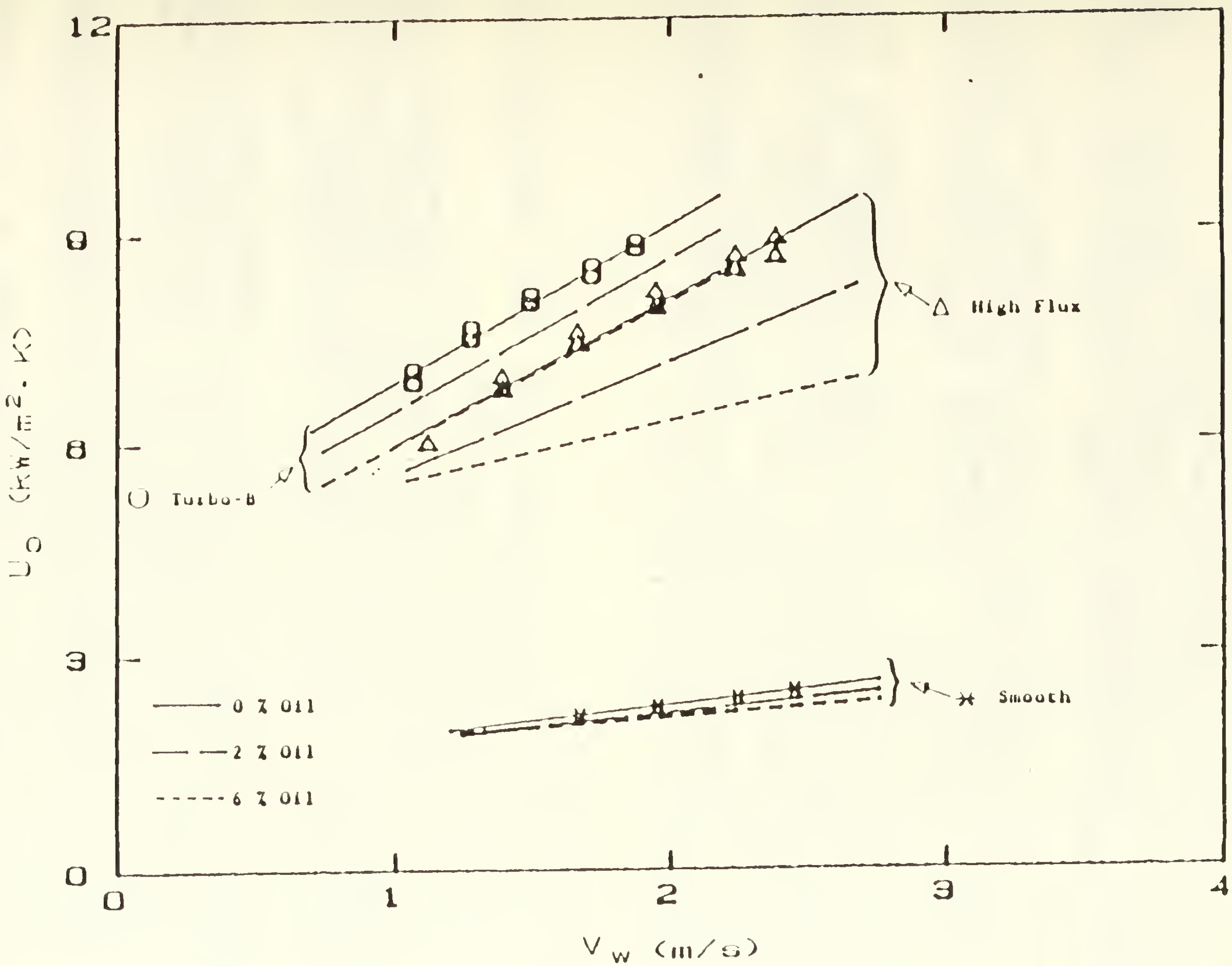

Figure 5.12. Variation of Overall Heat-Transfer Coefficient with Oil Mass Percent.

VI. CONCLUSIONS AND RECOMMENDATIONS

A. CONCLUSIONS

Considering the data gathered in this investigation for boiling of R-114 and oil mixtures at 13.8 °C boiling temperature, the following conclusions are reached:

1. Based on the overall heat-transfer coefficient, the Turbo-B and High Flux tubes outperformed the smooth tube by a factor greater than 3, and the Turbo-B tube outperformed the High Flux tube by a factor of 1.13.
2. At a heat flux of 40 kW/m^2 with zero mass percent oil, the outside coefficients of the High Flux and Turbo-B tubes were factors of 14.6 and 6.4 times, respectively, compared to the smooth tube. These factors decreased to 7.0 and 4.9 for the High Flux and Turbo-B tubes, respectively, with 6 mass percent oil.
3. The Turbo-B and High Flux tubes showed Sieder-Tate-type constants of 0.077 and 0.066, respectively, compared to the Sieder-Tate constant of 0.027 for long smooth tubes. As noted in the discussion, these values may be up to 10 percent lower for internally enhanced long tubes than the values for the short tubes.
4. While the High Flux tube outperformed the Turbo-B tube, based on the outside heat-transfer coefficient, the High Flux tube is more susceptible to the presence of oil.

B. RECOMMENDATIONS

Based on the results obtained from this investigation, the following recommendations are made:

1. The investigation of water-heated tubes should be upgraded to use long tubes. This would decrease the entrance effects that short tubes experience and it would come closer to duplicating actual operating conditions. Also, the pressure drop effect previously mentioned in Chapter V (RESULTS AND DISCUSSION) could be investigated in the analysis of the long tubes.
2. Studies of the boiling heat-transfer coefficients should be expanded to tube bundles. The interaction of tubes within the tube bundle is a major factor in the analysis of heat-transfer data. The boiling heat-transfer coefficient may be strongly influenced by any foaming action within the bundle.
3. Further investigations should be conducted on internal tube enhancements due to the major thermal resistance being the internal resistance.
4. Modifications to the condensing side of the present apparatus would allow for studies of short water-heated tubes at lower boiling temperatures. The major

modification would involve only the increase of the condenser drain piping to handle increases in the flow rate of the refrigerant liquid.

APPENDIX A
DATA REDUCTION PROGRAM

The data reduction program, DRP4, used for this investigation is listed below. A brief description of the major sections is given in Table 3, which is followed by an individual line listing of DRP4.

TABLE 3

DRP4 MAJOR SECTIONS

Line Number	Description
10-80	Selection options (i.e. process data, plot,etc.)
80-3690	Sub Program Main -boiling tube dimensions -select desired operating conditions (i.e. initiation mode, flow rate, Tsat, etc.) -convert emf's to temperatures -compute contact resistance (electrically heated mode only) -compute various water properties -various heat transfer calculations(Q, LMTD, U_o, etc.) -compute various Freon 114 properties -compute natural convective heat-transfer coefficient for unenhanced ends(iterative procedure) -compute heat loss for unenhanced ends -compute actual heat flux and boiling coefficient -record and store data
3700-4165	Functions for curve fits of various Freon 114 properties
4170-4220	Function for polynomial curve fit
4225-4935	Sub Program Poly -calculate nth order polynomial
4940-6175	Sub Program Plin -plot linear graphs
6180-6410	Sub Program Stats -calculate standard deviations
6415-6490	Sub Program Coeff -plot cross-plot files
6495-7280	Sub Program Wilson -calculate modified Wilson plot values (see Appx. C)
7285-7390	Functions for curve fits of various water properties
7395-9640	Sub Program Plot -plot non-linear graphs
9645-9725	Sub Program Symb -print various symbols on plotted graphs
9730-9755	Sub Program Purge -purge unwanted files
9760-10200	Sub Program Tdcn -calculate water temperature rise corrections due to pressure drop between thermopile locations
10205-10360	Sub Program U plot -print U_o files
10365-10475	Sub Program Select -select various sub program options

```
10   ! FILE NAME: DRP4
15   ! DATE:        October [illegible], 1984
20   ! REVISED:     April 07, 1986
25   !
30     COM /Idp/ Idp
35     PRINTER IS 1
40     CALL Select
45     INPUT "WANT TO SELECT ANOTHER OPTION (1=Y,0=N)?",Isel
50     IF Isel=1 THEN GOTO 40.
55     BEEP
60     BEEP
65     PRINTER IS 1
70     PRINT "DATA COLLECTION/REPROCESSING COMPLETED"
75     END
80     SUB Main
85     COM /Idp/ Idp
90     COM /Cc/ C(7),Ical
95     COM /Wil/ D2,Di,Do,L,Lu,Kcu
100    DIM Emf(12),T(12),D1a(9),D2a(9),Dia(9),Doa(9),La(9),Lua(9),Kcua(9),Et(19),
Tn$(4)[15]
105    DATA 0.10086091,25727.94369,-767345.8295,78025595.81
110    DATA -9247486589,6.97688E+11,-2.66192E+13,3.94078E+14
115    READ C(*)
120  ! DATA "Smooth","High Flux","Thermoexel-E","Thermoexel-HE"
125    DATA Smooth,High Flux,Turbo-B,High Flux Mod,Turbo-B Mod
130    READ Tn$(*)
135    PRINTER IS 701
140    BEEP
145    IF Idp=4 THEN PRINTER IS 1
150    IF Idp=4 THEN GOTO 1280
155    INPUT "ENTER MONTH, DATE AND TIME (MM:DD:HH:MM:SS)",Date$
160    OUTPUT 709:"TD":Date$
165    OUTPUT 709:"TD"
170    ENTER 709:Date$
175    PRINT
180    PRINT "            Month, date and time :":Date$
185    PRINT
190    PRINT USING "10X,""NOTE: Program name : DRP4"""
195    BEEP
200    INPUT "ENTER DISK NUMBER",Dn
205    PRINT USING "16X,""Disk number  = "",ZZ":Dn
210    BEEP
215    INPUT "ENTER INPUT MODE (0=3054A,1=FILE)",Im
220    BEEP
225    INPUT "SELECT HEATING MODE (0=ELEC; 1=WATER)",Ihm
230    BEEP
235    INPUT "ENTER THERMOCOUPLE TYPE (0=NEW,1=OLD)",Ical
240    IF Im=0 THEN
245    BEEP
250    INPUT "GIVE A NAME FOR THE RAW DATA FILE",D2_file$
255    PRINT USING "16X,""New file name: "",14A":D2_file$
260    Size1=20
265    CREATE BDAT D2_file$,Size1
270    ASSIGN @File2 TO D2_file$
275  !
280  ! DUMMY FILE UNTIL Nrun KNOWN
285    D1_file$="DUMMY"
290    CREATE BDAT D1_file$,Size1
295    ASSIGN @File1 TO D1_file$
```

```
300    OUTPUT @File1:Date$
305    IF Ihm=0 THEN
310    BEEP
315    INPUT "ENTER NUMBER OF DEFECTIVE TCS (0=DEFAULT)",Idtc
320    IF Idtc=0 THEN
325    Ldtc1=0
330    Ldtc2=0
335    PRINT USING "16X,""No defective TCs exist"""
340    END IF
345    IF Idtc=1 THEN
350    BEEP
355    INPUT "ENTER DEFECTIVE TC LOCATION",Ldtc1
360    PRINT USING "16X,""TC is defective at location "",D";Ldtc1
365    Ldtc2=0
370    END IF
375    IF Idtc=2 THEN
380    BEEP
385    INPUT "ENTER DEFECTIVE TC LOCATIONS",Ldtc1,Ldtc2
390    PRINT USING "16X,""TC are defective at locations "",D,4X,D";Ldtc1,Ldtc2
395    END IF
400    IF Idtc>2 THEN
405    BEEP
410    PRINTER IS 1
415    BEEP
420    PRINT "INVALID ENTRY"
425    PRINTER IS 701
430    GOTO 310
435    END IF
440    END IF
445    OUTPUT @File1:Ldtc1,Ldtc2
450  ! Im=1 option
455    ELSE
460    BEEP
465    INPUT "GIVE THE NAME OF THE EXISTING DATA FILE",D2_file$
470    PRINT USING "16X,""Old file name: "",14A";D2_file$
475    ASSIGN @File2 TO D2_file$
480    ENTER @File2:Nrun
485    ENTER @File2:Dold$
490    PRINT USING "16X,""This data set taken on : "",14A";Dold$
495    ENTER @File2:Ldtc1,Ldtc2
500    IF Ldtc1>0 OR Ldtc2>0 THEN
505    PRINT USING "16X,""Thermocouples were defective at locations:"",2(3D,4X)";
Ldtc1,Ldtc2
510    END IF
515    ENTER @File2:Itt
520    END IF
525  ! IF Im=0 AND Ihm=1 THEN !595
530    BEEP
535    INPUT "WANT TO CREATE A PLOT FILE? (0=N,1=Y)",Iplot
540    IF Iplot=1 THEN
545    BEEP
550    INPUT "GIVE NAME FOR PLOT FILE",P_file$
555    CREATE BDAT P_file$,4
560    ASSIGN @Plot TO P_file$
565    END IF
570    IF Ihm=1 THEN
575    BEEP
580    INPUT "WANT TO CREATE Uo FILE? (0=N,1=Y)",Iuf
585    IF Iuf=1 THEN
590    BEEP
```

```
595   INPUT "ENTER Jo FILE NAME",Jfile$
600   CREATE BDAT Jfile$,4
605   ASSIGN @Jfile TO Jfile$
610   END IF
615   BEEP
620   INPUT "WANT TO CREATE Re FILE? (0=N,1=Y)",Ire
625   IF Ire=1 THEN
630   BEEP
635   INPUT "ENTER Re FILE NAME",Refile$
640   CREATE BDAT Refile$,10
645   ASSIGN @Refile TO Refile$
650   END IF
655   END IF
660   PRINTER IS 1
665   IF Im=0 THEN
670   BEEP
675   PRINT USING "4X,""Select tube number"""
680   IF Ihm=0 THEN
685   PRINT USING "6X,""0  Smooth 4 inch Ref"""
690   PRINT USING "6X,""1  Smooth 4 inch Cu (Press/Slide)"""
695   PRINT USING "6X,""2  Soft Solder 4 inch Cu"""
700   PRINT USING "6X,""3  Soft Solder 4 inch HIGH FLUX"""
705   PRINT USING "6X,""4  Wieland Hard 8 inch"""
710   PRINT USING "6X,""5  HIGH FLUX 8 inch"""
715   PRINT USING "6X,""6  GEWA-K 19 Fins/in"""
720   PRINT USING "6X,""7  GEWA-K 26 Fins/in"""
725   PRINT USING "6X,""8  GEWA-T 19 Fins/in"""
730   PRINT USING "6X,""9  GEWA-T 26 Fins/in"""
735   ELSE
740   PRINT USING "6X,""0  Smooth tube"""
745   PRINT USING "6X,""1  High Flux"""
750   PRINT USING "6X,""2  Turbo-B"""
755   PRINT USING "6X,""3  High Flux Mod"""
760   PRINT USING "6X,""4  Turbo-B Mod"""
765   END IF
770   INPUT Itt
775   OUTPUT @File1:Itt
780   END IF
785   PRINTER IS 701
790   IF Itt<10 THEN PRINT USING "16X,""Tube Number:    "",D":Itt
795   IF Itt>9 THEN PRINT USING "16X,""Tube Number:    "",DD":Itt
800   IF Ihm=1 THEN PRINT USING "16X,""Tube Type:      "",15A":Tn$(Itt)
805   BEEP
810   INPUT "ENTER OUTPUT VERSION (0=LONG,1=SHORT,2=NONE)",Iov
815   BEEP
820   INPUT "SELECT (0=LIQ,1=VAP,2=(LIQ+VAP)/2)",Ilqv
825 !
830 ! DIMENSIONS FO TESTED TUBES
835 ! ELECTRIC HEATED MODE
840 ! D1=Diameter at thermocouple positions
845   DATA .0111125,.0111125,.0111125,.0129540,.012446,.0129540,.0100965
850   DATA .0100965,.01157,.01157
855   READ D1a(*)
860   D1=D1a(Itt)
865 !
870 ! D2=Diameter of test section to the base of fins
875   DATA .015875,.015875,.015875,.015824,.015875,.015824,.01270
880   DATA .0127,.0138,.0138
885   READ D2a(*)
890 !
895 ! Di=Inside diameter of unenhanced ends
```

```
900   DATA .0127,.0127,.0127,.0132,.0127,.0132,.01125,.01125,.0118,.0118
905   READ Dia(*)
910 !
915 ! Do=Outside diameter of unenhanced ends
920   DATA .015875,.015875,.015875,.015824,.015875,.015824,.01270,.01270,.01331,
.01331
925   READ Doa(*)
930 !
935 ! L=Length of enhanced surface
940   DATA .1016,.1016,.1016,.1016,.2032,.2032,.2032,.2032,.2032,.2032
945   READ La(*)
950 !
955 ! Lu=Length of unenhanced surface at the ends
960   DATA .0254,.0254,.0254,.0254,.0762,.0762,.0762,.0762,.0762,.0762
965   READ Lua(*)
970 !
975 ! Kcu=Thermal Conductivity of tube
980   DATA 398,344,344,45,344,45,344,944,398,398
985   READ Kcua(*)
990   IF Ihm=1 THEN
995 !
1000! Data statements for water heating mode
1005!
1010  DATA 0.015875,0.015875,0.0169,0.0138,0.0169,0,0,0,0,0
1015  READ D2a(*)
1020  DATA 0.0127,0.0127,0.0145,0.0127,0.0145,0,0,0,0,0
1025  READ Dia(*)
1030  DATA 0.015875,0.015875,0.0169,0.015875,0.0169,0,0,0,0,0
1035  READ Doa(*)
1040  DATA 0.3048,0.3048,0.3048,0.3048,0.3048,0,0,0,0,0
1045  READ La(*)
1050  DATA 0.0254,0.0254,0.0254,0.0254,0.0254,0,0,0,0,0
1055  READ Lua(*)
1060  DATA 398,45,398,45,398,0,0,0,0,0
1065  READ Kcua(*)
1070  END IF
1075  D2=D2a(Itt)
1080  Di=Dia(Itt)
1085  Do=Doa(Itt)
1090  L=La(Itt)
1095  Lu=Lua(Itt)
1100  Kcu=Kcua(Itt)
1105  Xn=.8
1110  Fr=.3
1115  IF Itt=0 THEN Cf=1.70E+9
1120  IF Itt>0 THEN Cf=3.7037E+10
1125  A=PI*(Do^2-Di^2)/4
1130  P=PI*Do
1135  BEEP
1140  INPUT "TUBE INITIATION MODE. (1=HOT WATER,2=STEAM,3=COLD WATER)",Itim
1145  IF Itim=1 THEN PRINT USING "16X,""Tube Initiate: Hot Water"""
1150  IF Itim=2 THEN PRINT USING "16X,""Tube Initiate: Steam"""
1155  IF Itim=3 THEN PRINT USING "16X,""Tube Initiate: Cold Water"""
1160  INPUT "TEMP/VEL MODE: (0=T-CONST,V-DEC:1=T-DEC,V-CONST: 2=T-INC,V-CONST)",
Itv
1165  IF Itv=0 THEN PRINT USING "16X,""Temp/Vel Mode: Constant/Decreasing"""
1170  IF Itv=1 THEN PRINT USING "16X,""Temp/Vel Mode: Decreasing/Constant"""
1175  IF Itv=2 THEN PRINT USING "16X,""Temp/Vel Mode: Increasing/Constant"""
1180  INPUT "WANT TO RUN WILSON PLOT? (1=Y,0=N)",Iwil
1185  IF Ihm=1 AND Iwil=0 THEN
```

```
1190  IF Itt=0 THEN Ci=.032
1195  IF Itt=1 OR Itt=3 THEN Ci=.059
1200  IF Itt=2 OR Itt=4 THEN Ci=.062
1205  BEEP
1210  INPUT "ENTER CI (DEF: NH=.032,HF=.059,TB=.062)",Ci
1215  PRINT USING "16X,""Sieder-Tate """
1220  PRINT USING "16X,""  Constant   = "",Z.4D";Ci
1225  END IF
1230  IF Ihm=1 AND Im=1 AND Iwil=1 THEN
1235  IF Itt=0 THEN Ci=.032
1240  IF Itt=1 OR Itt=3 THEN Ci=.059
1245  IF Itt=2 OR Itt=4 THEN Ci=.062
1250  ASSIGN @File2 TO *
1255  CALL Wilson(Cf,Ci)
1260  ASSIGN @File2 TO D2_file$
1265  ENTER @File2;Nrun,Dold$,Ldtc1,Ldtc2,Itt
1270  END IF
1275  Nsub=0
1280  IF Iap=4 THEN Ihm=1
1285  IF Ihm=1 THEN Nsub=8
1290  Ntc=6
1295  J=1
1300  Sx=0
1305  Sy=0
1310  Sxs=0
1315  Sxy=0
1320 Repeat: !
1325  IF Im=0 THEN
1330  Dtld=2.22
1335  Ido=2
1340  ON KEY 0,15 RECOVER 1320
1345  PRINTER IS 1
1350  PRINT USING "4X,""SELECT OPTION"""
1355  PRINT USING "6X,""0=TAKE DATA"""
1360  IF Ihm=0 THEN PRINT USING "6X,""1=SET HEAT FLUX"""
1365  IF Ihm=1 THEN PRINT USING "6X,""1=SET WATER FLOW RATE"""
1370  PRINT USING "6X,""2=SET Tsat"""
1375  PRINT USING "4X,""NOTE: KEY 0 = ESCAPE"""
1380  BEEP
1385  INPUT Ido
1390  IF Ido>2 THEN Ido=2
1395  IF Ido=0 THEN 2145
1400!
1405! LOOP TO SET HEAT FLUX OR FLOWMETER SETTING
1410  IF Ido=1 THEN
1415  IF Ihm=0 THEN
1420  OUTPUT 709;"AR AF12 AL13 VR5"
1425  BEEP
1430  INPUT "ENTER DESIRED Qdp",Qadp
1435  PRINT USING "4X,""DESIRED Qdp  ACTUAL Qdp"""
1440  Err=1000
1445  FOR I=1 TO 2
1450  OUTPUT 709;"AS SA"
1455  Sum=0
1460  FOR Ji=1 TO 5
1465  ENTER 709;E
1470  Sum=Sum+E
1475  NEXT Ji
1480  IF I=1 THEN Volt=Sum*5
1485  IF I=2 THEN Amp=E
```

```
1490  NEXT I
1495  Aaap=Volt*Amp/(PI*D2*L)
1500  IF ABS(Aaap-Daap)>Err THEN
1505  IF Aaap>Daap THEN
1510  BEEP 4000,.2
1515  BEEP 4000,.2
1520  BEEP 4000,.2
1525  ELSE
1530  BEEP 250,.2
1535  BEEP 250,.2
1540  BEEP 250,.2
1545  END IF
1550  PRINT USING "4X,MZ.3DE,2X,MZ.3DE";Dadp,Aadp
1555  WAIT 2
1560  GOTO 1445
1565  ELSE
1570  BEEP
1575  PRINT USING "4X,MZ.3DE,2X,MZ.3DE";Dadp,Aadp
1580  Err=500
1585  WAIT 2
1590  GOTO 1445
1595  END IF
1600  ELSE
1605  BEEP
1610  INPUT "ENTER FLOWMETER SETTING",Fms
1615  GOTO 1350
1620  END IF
1625  END IF
1630!
1635! LOOP TO SET Tsat
1640  IF Ido=2 THEN
1645  IF Ikdt=1 THEN 1670
1650  BEEP
1655  INPUT "ENTER DESIRED Tsat",Dtld
1660! PRINT USING "4X,""  DTsat   ATsat    Rate      Tv       Rate"""
1665  Ikdt=1
1670  Old1=0
1675  Old2=0
1680  Nn=1
1685  Nrs=Nn MOD 15
1690  Nn=Nn+1
1695  IF Nrs=1 THEN
1700  PRINT USING "4X,""   Tsat     Tld1      Tld2       Tv      Tsump    Tinlet     Tpile
   Tout"""
1705  END IF
1710  IF Ihm=0 THEN OUTPUT 709:"AR AF8 AL11 VR5"
1715  IF Ihm=1 THEN OUTPUT 709:"AR AF0 AL5 VR5"
1720  FOR I=1 TO 5
1725  IF Ihm=0 AND I>4 THEN 1860
1730  Sum=0
1735  OUTPUT 709:"AS SA"
1740  FOR Ji=1 TO 20
1745  ENTER 709:Eliq
1750  Sum=Sum+Eliq
1755  NEXT Ji
1760  Eliq=Sum/20
1765  Tld=FNTvsv(Eliq)
1770  IF I=1 THEN Tld1=Tld
1775  IF I=2 THEN Tld2=Tld
1780  IF I=3 THEN Tv=Tld
```

```
1785  IF I=4 THEN Tsump=Tld
1790  IF I=5 THEN Tinlet=Tld
1795  IF I=6 THEN Tout=Tld
1800  NEXT I
1805  IF Ihm=1 THEN
1810  OUTPUT 709:"AR AF20 AL20 VRS"
1815  OUTPUT 709:"AS SA"
1820  Sum=0
1825  FOR Kk=1 TO 20
1830  ENTER 709:E
1835  Sum=Sum+E
1840  NEXT Kk
1845  Emf(7)=ABS(Sum/20)
1850  Tpile=Emf(7)/3.96E-4
1855  END IF
1860  Atld=(Tld1+Tld2)*.5
1865  IF ABS(Atld-Dtld)>.2 THEN
1870  IF Atld>Dtld THEN
1875  BEEP 4000,.2
1880  BEEP 4000,.2
1885  BEEP 4000,.2
1890  ELSE
1895  BEEP 250,.2
1900  BEEP 250,.2
1905  BEEP 250,.2
1910  END IF
1915  Err1=Atld-Old1
1920  Old1=Atld
1925  Err2=Tv-Old2
1930  Old2=Tv
1935  IF Ihm=0 THEN PRINT USING "4X,5(MDD.DD,2X)":Dtld,Tld1,Tld2,Tv,Tsump
1940  IF Ihm=1 AND Idp=0 THEN PRINT USING "4X,7(MDD.DD,2X)";Dtld,Tld1,Tld2,Tv,Ts
ump,Tinlet,Tpile
1945+ IF Ihm=1 AND Idp=4 THEN PRINT USING "4X,5(MDD.DD,2X),3(M3D.DD,2X)":Dtld,Tl
d1,Tld2,Tv,Tsump,Tin
1950  WAIT 2
1955  GOTO 1685
1960  ELSE
1965  IF ABS(Atld-Dtld)>.1 THEN
1970  IF Atld>Dtld THEN
1975  BEEP 3000,.2
1980  BEEP 3000,.2
1985  ELSE
1990  BEEP 800,.2
1995  BEEP 800,.2
2000  END IF
2005  Err1=Atld-Old1
2010  Old1=Atld
2015  Err2=Tv-Old2
2020  Old2=Tv
2025  IF Ihm=0 THEN PRINT USING "4X,5(MDD.DD,2X)":Dtld,Tld1,Tld2,Tv,Tsump
2030+ IF Ihm=1 THEN PRINT USING "4X,5(MDD.DD,2X),3(M3D.DD,1X)":Dtld,Tld1,Tld2,Tv
,Tsump,Tinlet,Tpile,
2035  WAIT 2
2040  GOTO 1685
2045  ELSE
2050  BEEP
2055  Err1=Atld-Old1
2060  Old1=Atld
2065  Err2=Tv-Old2
```

```
2070  Dld2=Tv
2075  IF Ihm=0 THEN PRINT USING "4X.5(MDD.DD.2X)":Dtld.Tld1.Tld2.Tv.Tsump
2080  IF Ihm=1 THEN PRINT USING "4X.8(MDD.DD.2X)":Dtld.Tld1.Tld2.Tv.Tsump.Tinlet
.Tpile.Tout
2085  WAIT 2
2090  GOTO 1685
2095  END IF
2100  END IF
2105  END IF
2110! ERROR TRAP FOR Ido OUT OF BOUNDS
2115  IF Ido>2 THEN
2120  BEEP
2125  GOTO 1350
2130  END IF
2135!
2140! TAKE DATA IF Im=0 LOOP
2145  IF Ikol=1 THEN 2165
2150  BEEP
2155  INPUT "ENTER BULK OIL %".Bop
2160  Ikol=1
2165  IF Ihm=0 THEN OUTPUT 709:"AR AF0 AL11 VR5"
2170  IF Ihm=1 THEN OUTPUT 709:"AR AF0 AL5 VR5"
2175  IF Ihm=0 THEN Ntc=12
2180  FOR I=1 TO Ntc
2185  OUTPUT 709:"AS SA"
2190  Sum=0
2195  FOR Ji=1 TO 20
2200  ENTER 709:E
2205  Sum=Sum+E
2210  IF I=(9-Nsub) OR I=(10-Nsub) THEN Et(Ji-1)=E
2215  NEXT Ji
2220  Kdl=0
2225  IF I=(9-Nsub) OR I=(10-Nsub) THEN
2230  Eave=Sum/20
2235  Sum=0.
2240  FOR Jk=0 TO 19
2245  IF ABS(Et(Jk)-Eave)<5.0E-6 THEN
2250  Sum=Sum+Et(Jk)
2255  ELSE
2260  Kdl=Kdl+1
2265  END IF
2270  NEXT Jk
2275  IF I=(9-Nsub) OR I=(10-Nsub) THEN PRINT USING "4X.""Kdl = "".DD":Kdl
2280  IF Kdl>10 THEN
2285  BEEP
2290  BEEP
2295  PRINT USING "4X.""Too much scattering in data - repeat data set"""
2300  GOTO 1345
2305  END IF
2310  END IF
2315  Emf(I)=Sum/(20-Kdl)
2320  NEXT I
2325  IF Ihm=1 THEN
2330  OUTPUT 709:"AR AF20 AL20 VR5"
2335  OUTPUT 709:"AS SA"
2340  Sum=0
2345  FOR Kk=1 TO 20
2350  ENTER 709:E
2355  Sum=Sum+E
2360  NEXT Kk
2365  Emf(7)=ABS(Sum)/20
```

```
2370  END IF
2375  IF Ihm=0 THEN
2380  OUTPUT 709:"AR AF12 AL13 VR5"
2385  FOR I=1 TO 2
2390  OUTPUT 709:"AS SA"
2395  Sum=0
2400  FOR J1=1 TO 2
2405  ENTER 709:E
2410  Sum=Sum+E
2415  NEXT J1
2420  IF I=1 THEN Vr=Sum/2
2425  IF I=2 THEN Ir=Sum/2
2430  NEXT I
2435  END IF
2440  ELSE
2445  IF Ihm=0 THEN ENTER @File2:Bop,Told$,Emf(*),Vr,Ir
2450  IF Ihm=1 THEN ENTER @File2:Bop,Told$,Emf(*),Fms
2455  END IF
2460!
2465! CONVERT emf'S TO TEMP.VOLT.CURRENT
2470  Twa=0
2475  FOR I=1 TO Ntc
2480  IF Idtc>0 THEN
2485  IF I=Ldtc1 OR I=Ldtc2 THEN
2490  T(I)=-99.99
2495  GOTO 2545
2500  END IF
2505  END IF
2510  IF Itt<4 AND Ihm=0 THEN
2515  IF I>4 AND I<9 THEN
2520  T(I)=-99.99
2525  GOTO 2545
2530  END IF
2535  END IF
2540  T(I)=FNTvsv(Emf(I))
2545  NEXT I
2550  IF Itt<4 THEN
2555  FOR I=1 TO 4
2560  IF I=Ldtc1 OR I=Ldtc2 THEN
2565  Twa=Twa
2570  ELSE
2575  Twa=Twa+T(I)
2580  END IF
2585  NEXT I
2590  Twa=Twa/(4-Idtc)
2595  ELSE
2600  IF Ihm=1 THEN 2650
2605  FOR I=1 TO 8
2610  IF I=Ldtc1 OR I=Ldtc2 THEN
2615  Twa=Twa
2620  ELSE
2625  Twa=Twa+T(I)
2630  END IF
2635  NEXT I
2640  Twa=Twa/(8-Idtc)
2645  END IF
2650  Tld=T(9-Nsup)
2655  Tld2=T(10-Nsup)
2660  Tlda=(Tld+Tld2)*.5
2665  Tv=T(11-Nsup)
```

```
2670  IF Itt<3 AND Ihm=0 THEN
2675  Tld2=-99.99
2680  Tv=(T(10)+T(11))/2
2685  END IF
2690  IF Ihm=0 THEN 2710
2695  Tsump=T(12-Nsup)
2700  Tinlet=T(13-Nsup)
2705  Tout=T(14-Nsup)
2710  IF Ihm=0 THEN
2715  Amp=ABS(Ir)
2720  Volt=ABS(Vr)*25
2725  Q=Volt*Amp
2730  END IF
2735  IF Itt=0 AND Ihm=0 THEN
2740  Kcu=FNKcu(Twa)
2745  ELSE
2750  Kcu=Kcua(Itt)
2755  END IF
2760!
2765! FOURIER CONDUCTION EQUATION WITH CONTACT RESISTANCE NEGLECTED
2770  IF Ihm=0 THEN Tw=Twa-Q*LOG(D2/D1)/(2*PI*Kcu*L)
2775  IF Ilqv=0 THEN Tsat=Tlda
2780  IF Ilqv=1 THEN Tsat=(Tlda+Tv)*.5
2785  IF Ilqv=2 THEN Tsat=Tv
2790  IF Ihm=1 THEN
2795  Tavg=Tinlet
2800  Grad=37.9853+.104388*Tavg
2805  Tdrop=ABS(Emf(7))*1.E+6/(10*Grad)
2810  Tavgc=Tinlet-Tdrop*.5
2815  IF ABS(Tavg-Tavgc)>.01 THEN
2820  Tavg=(Tavg+Tavgc)*.5
2825  GOTO 2800
2830  END IF
2835!
2840! COMPUTE WATER PROPERTIES
2845  Kw=FNKw(Tavg)
2850  Muwa=FNMuw(Tavg)
2855  Cpw=FNCpw(Tavg)
2860  Prw=FNPrw(Tavg)
2865  Rhow=FNRhow(Tavg)
2870  Twi=Tavg
2875!
2880! Compute MDOT
2885  Mdot=3.9657E-3+Fms*(3.61955E-3-Fms*(3.82006E-6-Fms*(1.23688E-7-Fms*4.31897
E-10)))
2890! Mdot=Mdot*(1.0365-Tinlet*(1.36644E-3-Tinlet*5.252E-6))/1.0037
2895  Kdt=0
2900  Q=Mdot*Cpw*Tdrop
2905  Lmtd=Tdrop/LOG((Tinlet-Tsat)/(Tinlet-Tdrop-Tsat))
2910  Uo=Q/(PI*Do*L*Lmtd)
2915  Rw=Do*LOG(Do/Di)/(2.*Kcu)
2920  Tw=Tsat+Fr*Lmtd
2925  Vw=Mdot/(Rhow*PI*Di^2/4)
2930! IF Kdt=0 THEN
2935! Kdt=1
2940! Tdrop=Tdrop-.004*Vw^2
2945! GOTO 3710
2950! END IF
2955  Rew=Rhow*Vw*Di/Muwa
2960  Hi=Ci*Kw/Di*Rew^.8*Prw^(1/3.)*(Muwa/FNMuw(Twi))^.14
2965  Twic=Tavg-Q/(PI*Do*L*Hi)
```

```
2970  IF ABS(Twi-Twic)>.01 THEN
2975  Twi=(Twi+Twic)*.5
2980  GOTO 2960
2985  END IF
2990  Twi=(Twi+Twic)*.5
2995  Ho=1/(1/Uo-Do/(Di*Hi)-Rw)
3000  Thetap=Q/(Ho*PI*Do*L)
3005  Tw=Tsat+Thetap
3010  Thetap=Tw-Tsat
3015  IF Thetap<0 THEN
3020  BEEP
3025  INPUT "TWALL<TSAT (0=CONTINUE, 1=END)",Iev
3030  IF Iev=0 THEN GOTO 1325
3035  IF Iev=1 THEN 3535
3040  END IF
3045  END IF
3050!
3055! COMPUTE VARIOUS PROPERTIES
3060  Tfilm=(Tw+Tsat)*.5
3065  Rho=FNRho(Tfilm)
3070  Mu=FNMu(Tfilm)
3075  K=FNK(Tfilm)
3080  Cp=FNCp(Tfilm)
3085  Beta=FNBeta(Tfilm)
3090  Hfg=FNHfg(Tsat)
3095  Ni=Mu/Rho
3100  Alpha=K/(Rho*Cp)
3105  Pr=Ni/Alpha
3110  Psat=FNPsat(Tsat)
3115!
3120! COMPUTE NATURAL-CONVECTIVE HEAT-TRANSFER COEFFICIENT
3125! FOR UNENHANCED END(S)
3130  Hbar=190
3135  Fe=(Hbar*P/(Kcu*A))^.5*Lu
3140  Tanh=FNTanh(Fe)
3145  Theta=Thetap*Tanh/Fe
3150  Xx=(9.81*Beta*Thetap*Do^3*Tanh/(Fe*Ni*Alpha))^.166667
3155  Yy=(1+(.559/Pr)^(9/16))^(8/27)
3160  Hbarc=K/Do*(.6+.387*Xx/Yy)^2
3165  IF ABS((Hbar-Hbarc)/Hbarc)>.001 THEN
3170  Hbar=(Hbar+Hbarc)*.5
3175  GOTO 3135
3180  END IF
3185!
3190! COMPUTE HEAT LOSS RATE THROUGH UNENHANCED END(S)
3195  Q1=(Hbar*P*Kcu*A)^.5*Thetap*Tanh
3200  Qc=Q-2*Q1
3205  As=PI*D2*L
3210!
3215! COMPUTE ACTUAL HEAT FLUX AND BOILING COEFFICIENT
3220  Qdp=Qc/As
3225  Htube=Qdp/Thetap
3230  Csf=(Cp*Thetap/Hfg)/(Qdp/(Mu*Hfg)*(.014/(9.81*Rho)^.5)^(1/3.)*Pr^1.7)
3235!
3240! RECORD TIME OF DATA TAKING
3245  IF Im=0 THEN
3250  OUTPUT 709:"TD"
3255  ENTER 709:Told$
3260  END IF
3265!
```

```
3270! OUTPUT DATA TO PRINTER
3275  PRINTER IS 701
3280  IF Iov=0 THEN
3285  PRINT
3290  PRINT USING "10X,""Data Set Number = "",DDD,2X,""Bulk Oil % = "",DD.D,5X,1
4A";J,Bop,Told$
3295  IF Ihm=0 THEN
3300  PRINT USING "10X,""TC No:     1       2       3       4       5       6       7
    8"""""
3305  PRINT USING "10X,""Temp :"",8(1X,MDD.DD)";T(1),T(2),T(3),T(4),T(5),T(6),T(
7),T(8)
3310  PRINT USING "10X,"" Twa     Tliqd   Tliqd2  Tvapr  Psat    Tsump"""""
3315  PRINT USING "10X,2(MDD.DD,1X),1X,MDD.DD,1X,2(1X,MDD.DD),2X,MDD.D";Twa,Tld,
Tld2,Tv,Psat,Tsump
3320  PRINT USING "10X,"" Thetab  Htube       Qdp"""""
3325  PRINT USING "10X,MDD.3D,1X,MZ.3DE,1X,MZ.3DE";Thetab,Htube,Qdp
3330  ELSE
3335  PRINT USING "10X,"" Fms     Vw    Tsat  Tinl Tdrop Thetab      q           Uo
    Ho"""""
3340* PRINT USING "10X,4(2D.DD,1X),Z.3D,1X,DD.DD,1X,3(MZ.3DE,1X)";Fms,Vw,Tsat,Ti
nlet,Tdrop,Thetab,Qd
3345  END IF
3350  END IF
3355  IF Iov=1 THEN
3360  IF J=1 THEN
3365  PRINT
3370  IF Ihm=0 THEN
3375  PRINT USING "10X,"" RUN No  Oil%  Tsat    Htube       Qdp         Thetab"""""
3380  ELSE
3385  PRINT USING "10X,""  FMS    OIL%  TSAT    HTUBE       QDP         THETAB"""""
3390  END IF
3395  END IF
3400  IF Ihm=0 THEN
3405  PRINT USING "12X,3D,4X,DD,2X,MDD.DD,3(1X,MZ.3DE)";J,Bop,Tsat,Htube,Qdp,The
tab
3410  ELSE
3415  PRINT USING "12X,3D,4X,DD,2X,MDD.DD,3(1X,MZ.3DE)";Fms,Bop,Tsat,Htube,Qdp,T
hetab
3420  END IF
3425  END IF
3430  IF Im=0 THEN
3435  BEEP
3440  INPUT "OK TO STORE THIS DATA SET (1=Y,0=N)?",Ok
3445  END IF
3450  IF Ok=1 OR Im=1 THEN J=J+1
3455  IF Ok=1 AND Im=0 THEN
3460  IF Ihm=0 THEN OUTPUT @File1;Bop,Told$,Emf(*),Vr,Ir
3465  IF Ihm=1 THEN OUTPUT @File1;Bop,Told$,Emf(*),Fms
3470  END IF
3475  IF Iuf=1 THEN OUTPUT @Ufile;Vw,Uo
3480  IF Ire=1 THEN OUTPUT @Refile;Fms,Rew
3485  IF (Im=1 OR Ok=1) AND Iplot=1 THEN OUTPUT @Plot;Qdp,Thetab
3490  IF Im=0 THEN
3495  BEEP
3500  INPUT "WILL THERE BE ANOTHER RUN (1=Y,0=N)?",Go_on
3505  Nrun=J
3510  IF Go_on=0 THEN 3535
3515  IF Go_on<>0 THEN Repeat
3520  ELSE
3525  IF J<Nrun+1 THEN Repeat
3530  END IF
```

```
3535  IF Im=0 THEN
3540  BEEP
3545  PRINT USING "10X,""NOTE: "",ZZ,"" data runs were stored in file "",10A":J-1,D2_file$
3550  ASSIGN @File1 TO *
3555  OUTPUT @File2:Nrun-1
3560  ASSIGN @File1 TO D1_file$
3565  ENTER @File1:Date$,Ldtc1,Ldtc2,Itt
3570  OUTPUT @File2:Date$,Ldtc1,Ldtc2,Itt
3575  FOR I=1 TO Nrun-1
3580  IF Ihm=0 THEN
3585  ENTER @File1:Bop,Told$,Emf(*),Vr,Ir
3590  OUTPUT @File2:Bop,Told$,Emf(*),Vr,Ir
3595  ELSE
3600  ENTER @File1:Bop,Told$,Emf(*),Fms
3605  OUTPUT @File2:Bop,Told$,Emf(*),Fms
3610  END IF
3615  NEXT I
3620  ASSIGN @File1 TO *
3625  PURGE "DUMMY"
3630  END IF
3635  BEEP
3640  PRINT
3645* IF Iplot=1 THEN PRINT USING "10X,""NOTE: "",ZZ,"" X-Y pairs were stored in plot data file "",1
3650  ASSIGN @File2 TO *
3655  ASSIGN @Plot TO *
3660  IF Iuf=1 THEN ASSIGN @Ufile TO *
3665  IF Ire=1 THEN ASSIGN @Refile TO *
3670  CALL Stats
3675  BEEP
3680  INPUT "LIKE TO PLOT DATA (1=Y,0=N)?",Ok
3685  IF Ok=1 THEN CALL Plot
3690  SUBEND
3695!
3700! CURVE FITS OF PROPERTY FUNCTIONS
3705  DEF FNKcu(T)
3710! OFHC COPPER 250 TO 300 K
3715  Tk=T+273.15      !C TO K
3720  K=434-.112*Tk
3725  RETURN K
3730  FNEND
3735  DEF FNMu(T)
3740! 170 TO 360 K CURVE FIT OF VISCOUSITY
3745  Tk=T+273.15      !C TO K
3750  Mu=EXP(-4.4636+(1011.47/Tk))*1.0E-3
3755  RETURN Mu
3760  FNEND
3765  DEF FNCp(T)
3770! 180 TO 400 K CURVE FIT OF Cp
3775  Tk=T+273.15      !C TO K
3780  Cp=.40188+1.650075E-3*Tk+1.51494E-6*Tk^2-6.67853E-10*Tk^3
3785  Cp=Cp*1000
3790  RETURN Cp
3795  FNEND
3800  DEF FNRho(T)
3805  Tk=T+273.15      !C TO K
3810  X=1-(1.8*Tk/753.35)  !K TO R
3815  Ro=36.32+61.146414*X^(1/3)+16.418015*X+17.476838*X^.5+1.119828*X^2
3820  Ro=Ro/.062428
3825  RETURN Ro
```

```
3830  FNEND
3835  DEF FNPr(T)
3840  Pr=FNCp(T)*FNMu(T)/FNK(T)
3845  RETURN Pr
3850  FNEND
3855  DEF FNK(T)
3860! T<360 K WITH T IN C
3865  K=.071-.000261*T
3870  RETURN K
3875  FNEND
3880  DEF FNTanh(X)
3885  P=EXP(X)
3890  Q=1/P
3895  Tanh=(P-Q)/(P+Q)
3900  RETURN Tanh
3905  FNEND
3910  DEF FNTvsv(V)
3915  COM /Cc/ C(7),Ical
3920  T=C(0)
3925  FOR I=1 TO 7
3930  T=T+C(I)*V^I
3935  NEXT I
3940  IF Ical=1 THEN
3945  T=T-6.7422934E-2+T*(9.0277043E-3-T*(-9.3259917E-5))
3950  ELSE
3955  T=T+8.626897E-2+T*(3.76199E-3-T*5.0689259E-5)
3960  END IF
3965  RETURN T
3970  FNEND
3975  DEF FNBeta(T)
3980  Rop=FNRho(T+.1)
3985  Rom=FNRho(T-.1)
3990  Beta=-2/(Rop+Rom)*(Rop-Rom)/.2
3995  RETURN Beta
4000  FNEND
4005  DEF FNHfg(T)
4010  Hfg=1.3741344E+5-T*(3.3094361E-2+T*1.2165143)
4015  RETURN Hfg
4020  FNEND
4025  DEF FNPsat(Tc)
4030! 0 TO 80 deg F CURVE FIT OF Psat
4035  Tf=1.8*Tc+32
4040  Pa=5.945525+Tf*(.15352082+Tf*(1..4840963E-3+Tf*9.6150671E-6))
4045  Pg=Pa-14.7
4050  IF Pg>0 THEN       ! +=PSIG,-=in Hg
4055  Psat=Pg
4060  ELSE
4065  Psat=Pg*29.92/14.7
4070  END IF
4075  RETURN Psat
4080  FNEND
4085  DEF FNHsmooth(X,Bop,Isat)
4090  DIM A(5),B(5),C(5),D(5)
4095  DATA .20526,.25322,.319048,.55322,.79909,1.00258
4100  DATA .74515,.72992,.73189,.71225,.68472,.64197
4105  DATA .41092,.17725,.25142,.54806,.81916,1.0845
4110  DATA .71403,.72913,.72565,.696691,.665867,.61889
4115  READ A(*),B(*),C(*),D(*)
4120  IF Bop<6 THEN I=Bop
4125  IF Bop=6 THEN I=4
```

```
4130  IF Bop=10 THEN I=5
4135  IF Isat=1 THEN
4140  Hs=EXP(A(I)+B(I)*LOG(X))
4145  ELSE
4150  Hs=EXP(C(I)+D(I)*LOG(X))
4155  END IF
4160  RETURN Hs
4165  FNEND


6495  SUB Wilson(Cf.Ci)
6500  COM /Wil/ D2.Di.Do.L.Lu.Kcu
6505  DIM Emf(12)
6510! WLISON PLOT SUBROUTINE DETERMINE CF AND CI
6515  BEEP
6520  INPUT "ENTER DATA FILE NAME".Files
6525  BEEP
6530  PRINTER IS 1
6535  PRINT USING "4X.""Select option:"""
6540  PRINT USING "4X.""  0 Vary Cf and  Ci"""
6545  PRINT USING "4X.""  1 Fix  Cf Vary Ci"""
6550  PRINT USING "4X.""  2 Vary Cf Fix  Ci"""
6551  PRINT USING "4X.""  3 Fix  Cf Fix  Ci"""
6555  INPUT "ENTER OPTION".Icfix
6560  PRINTER IS 701
6565  IF Icfix=0 THEN 6585
6570  IF Icfix>0 THEN BEEP
6575  IF Icfix=1 THEN INPUT "ENTER Cf".Csf
6580  IF Icfix=2 THEN INPUT "ENTER CI".Ci
6581  IF Icfix=3 THEN INPUT "ENTER Cf. Ci".Csf.Ci
6585  PRINTER IS 1
6590  INPUT "Want To Vary Coeff?(1=Y.0=N)".Iccoef
6595  IF Iccoef=1 THEN INPUT "ENTER COEFF".R
6600  PRINTER IS 701
6605  IF Icfix=0 OR Icfix=2 THEN Cfa=.004
6610  IF Icfix=1 THEN Cfa=Csf
6615  Cia=Ci
6620  Xn=.8
6625  Fr=.3
6630  Jj=0
6635  Rr=3.
6640  IF Iccoef=1 THEN Rr=R
6645  PRINTER IS 1
6650  PRINT Do.Di.Kcu
6655  ASSIGN @File TO Files
6660  ENTER @File:Nrun.Date$.Ldtc1.Ldtc2.Itt
6665  Rw=Do*LOG(Do/Di)/(2*Kcu)
6670  Sx=0
6675  Sy=0
6680  Sxy=0
6685  Sx2=0
6690  Sy2=0
6695  FOR I=1 TO Nrun
6700  ENTER @File:Bop.Told$.Emf(*).Fms
6705! CONVERT EMF'S TO TEMPERATURE
6710  FOR J=1 TO 5
6715  T(J)=FNTvsv(Emf(J))
6720  NEXT J
6725  Tsat=(T(1)+T(2))*.5
6730  Tavg=T(5)
```

```
6735  Grad=37.3853+.104388*Tavg
6740  Tdrop=Emf(7)*1.E+6/(10.*Grad)
6745  Tavgc=T(5)-Tdrop*.5
6750  IF ABS(Tavg-Tavgc)>.01 THEN
6755  Tavg=(Tavg+Tavgc)*.5
6760  GOTO 6735
6765  END IF
6770!
6775! Compute properties of water
6780  Kw=FNKw(Tavg)
6785  Muwa=FNMuw(Tavg)
6790  Cpw=FNCpw(Tavg)
6795  Prw=FNPrw(Tavg)
6800  Rhow=FNRhow(Tavg)
6805!
6810! Compute properties of Freon-114
6815  Lmtd=Tdrop/LOG((T(5)-Tsat)/(T(5)-Tdrop-Tsat))
6820  IF Jj=0 THEN
6825  Tw=Tsat+Fr*Lmtd
6830  Thetab=Tw-Tsat
6835  Jj=1
6840  END IF
6845  Tf=(Tw+Tsat)*.5
6850  Rho=FNRho(Tf)
6855  Mu=FNMu(Tf)
6860  K=FNK(Tf)
6865  Cp=FNCp(Tf)
6870  Beta=FNBeta(Tf)
6875  Hfg=FNHfg(Tsat)
6880  Ni=Mu/Rho
6885  Alpha=K/(Rho*Cp)
6890  Pr=Ni/Alpha
6895!
6900! Analysis
6905! COMPUTE MDOT
6910  A=PI*(Do^2-Di^2)/4
6915  P=PI*Do
6920  Mdot=3.9657E-3+Fms*(3.61955E-3-Fms*(8.32006E-6-Fms*(1.23688E-7-Fms*4.31897
E-10)))
6925  Q=Mdot*Cpw*Tdrop
6930! COMPUTE NATURAL-CONVECTIVE HEAT-TRANSFER COEFFICIENT
6935! FOR UNENHANCED END(S)
6940  Hbar=190
6945  Fe=(Hbar*P/(Kcu*A))^.5*Lu
6950  Tanh=FNTanh(Fe)
6955  Theta=Thetap*Tanh/Fe
6960  Xx=(9.81*Beta*Thetap*Do^3*Tanh/(Fe*Ni*Alpha))^.166667
6965  Yy=(1+(.559/Pr)^(9/16))^(8/27)
6970  Hbarc=K/Do*(.6+.387*Xx/Yy)^2
6975  IF ABS((Hbar-Hbarc)/Hbar)>.001 THEN
6980  Hbar=(Hbar+Hbarc)*.5
6985  GOTO 6945
6990  END IF
6995!
7000! COMPUTE HEAT LOSS RATE THROUGH UNENHANCED ENDS
7005  Q1=(Hbar*P*Kcu*A)^.5*Thetap*Tanh
7010  Qc=Q-2*Q1
7015  As=PI*D2*L
7020! COMPUTE ACTUAL HEAT FLUX
7025  Qdp=Qc/As
```

```
7030  IF Icfix=0 OR Icfix=2 THEN Csf=1/Cf (1./Rr)
7035  Thetap=Csf/Cp*Hfg*(Qdp/(Mu*Hfg)*(.074/(9.81*Rho)) .5) (1/Rr)*Pr 1.7
7040  Ho=Qdp/Thetap
7045  Omega=Ho/Cf
7050  Uo=Q/(PI*Do*L*Lmtd)
7055  Vw=Mdot/(Rhow*PI*Di^2/4)
7060  Rew=Rhow*Vw*Di/Muwa
7065  Twi=Tw+Q*Rw/(PI*Do*L)
7070  Gama=Kw/Di*Rew^.8*Prw (1/3.)*(Muwa/FNMuw(Twi))^.14
7075! PRINTER IS 1
7080  Yw=(1./Uo-Rw)*Omega
7085  Xw=Omega*Do/(Gama*Di)
7090  Sx=Sx+Xw
7095  Sy=Sy+Yw
7100  Sxy=Sxy+Yw*Xw
7105  Sx2=Sx2+Xw*Xw
7110  Sy2=Sy2+Yw*Yw
7115  NEXT I
7120  ASSIGN @File TO *
7125  M=(Sx*Sy-Nrun*Sxy)/(Sx*Sx-Nrun*Sx2)
7130  C=(Sy-Sx*M)/Nrun
7135  IF Icfix=0 OR Icfix=3 OR Icfix=4 THEN
7140  Cic=1/M
7145  Cfc=1/C
7150  END IF
7155  IF Icfix=1 THEN
7160  Cic=1/M
7165  Cfc=Cf
7170  END IF
7175  IF Icfix=2 THEN
7180  Cic=Ci
7185  Cfc=1/C
7190  END IF
7191  IF Icfix=3 THEN 7280
7195  IF ABS((Ci-Cic)/Cic)>.001 OR ABS((Cf-Cfc)/Cfc)>.001 THEN
7200  Ci=(Ci+Cic)*.5
7205  Cf=(Cf+Cfc)*.5
7210  PRINTER IS 1
7215  PRINT USING "2X,"" Csf = "",MZ.3DE,2X,"" Ci = "",MZ.3DE":Csf,Ci
7220  PRINTER IS 701
7225  GOTO 6655
7230  END IF
7235  PRINT
7240  PRINTER IS 701
7245  PRINT USING "23X,""  Cf              Ci"""
7250  PRINT USING "3X,""ASSUMED    .    "",MZ.3DE,3X,MZ.3DE":Cfa,Cia
7255  PRINT USING "3X,""CALCULATED      "",MZ.3DE,3X,MZ.3DE":Csf,Ci
7260  PRINT
7265  Sum2=Sy2-2*M*Sxy-2*C*Sy+M^2*Sx2+2*M*C*Sx+Nrun*C^2
7270  PRINT USING "10X,""Sum of Squares = "",Z.3DE":Sum2
7275  PRINT USING "10X,""Coefficient = "",D.DDD":Rr
7280  SUBEND
7285  DEF FNMuw(T)
7290  A=247.8/(T+133.15)
7295  Mu=2.4E-5*10^A
7300  RETURN Mu
7305  FNEND
7310  DEF FNCpw(T)
7315  Cpw=4.21120858-T*(2.26826E-3-T*(4.42061E-5+2.71428E-7*T))
7320  RETURN Cpw*1000
7325  FNEND
```

```
7330  DEF FNRhow(T)
7335  Ro=999.52946+T*(.01269-T*(5.482513E-3-T*1.234147E-5))
7340  RETURN Ro
7345  FNEND
7350  DEF FNPrw(T)
7355  Prw=FNCpw(T)*FNMuw(T)/FNKw(T)
7360  RETURN Prw
7365  FNEND
7370  DEF FNKw(T)
7375  X=(T+273.15)/273.15
7380  Kw=-.92247+X*(2.8395-X*(1.3007-X*(.52577-.07344*X)))
7385  RETURN Kw
7390  FNEND


10365 SUB Select
10370 COM /Idp/ Idp
10375 BEEP
10380 PRINTER IS 1
10385 PRINT USING "4X,""Select option:"""
10390 PRINT USING "6X,""0 Taking data or re-processing previous data"""
10395 PRINT USING "6X,""1 Plotting data on Log-Log """
10400 PRINT USING "6X,""2 Plotting data on Linear"""
10405 PRINT USING "6X,""3 Make cross-plot coefft file"""
10410 PRINT USING "6X,""4 Re-circulate water"""
10415 PRINT USING "6X,""5 Purge"""
10420 PRINT USING "6X,""6 T-Drop correction"""
10425 PRINT USING "6X,""7 Print Uo File"""
10430 INPUT Idp
10435 IF Idp=0 THEN CALL Main
10440 IF Idp=1 THEN CALL Plot
10445 IF Idp=2 THEN CALL Plin
10450 IF Idp=3 THEN CALL Coef
10455 IF Idp=4 THEN CALL Main
10460 IF Idp=5 THEN CALL Purg
10465 IF Idp=6 THEN CALL Tdcn
10470 IF Idp=7 THEN CALL Uoprt
10475 SUBEND
```

APPENDIX B

FLOWMETER CALIBRATION

A Fischer Porter Flowmeter was used in the experimental apparatus to indicate the water flowrate. Prior to conducting the boiling tube data runs, calibration of the flowmeter was performed over a temperature range from 19 °C to 38 °C. The goals of the calibration were:

1) to develop a mathematical expression relating flowmeter percent reading to mass flowrate and
2) to determine a viscosity correction factor due to varying temperature range and flowrates.

A weigh tank, platform-type scale, and stopwatch were used to record water collection data.

Data were processed using the program "FMCAL", listed later in this appendix. This program took the flowmeter percent reading, water weight collected, and elapsed water collection time as the inputs. The outputs were an experimental mass flowrate and a mass flowrate difference. This difference was given by a mass flowrate computed from a correlation minus the experimental mass flow rate for the same flowmeter percent reading. The correlation was based on a fourth-order least-squares fit to the calibration data. After all the data runs were completed, the data points were combined into one file and a single fourth-order polynomial was generated to describe the relationship between the flowmeter percent reading and the mass flowrate. Of the original data points, 98.61 percent were within a ± 5.5 percent range. Reprocessing the data points led to 78 percent within a ± 1.02 percent range. The equation (B.1), resulting from the calibration data analysis, is a fourth-order polynomial from a curve fit of the reprocessed data without a viscosity correction factor:

$$\dot{m} = 3.9657e{-3} + 3.1690e{-3}(FMS) - 8.8020e{-6}(FMS)^2 + 1.2369e{-7}(FMS)^3 - 4.3190e{-10}(FMS)^4 \qquad (B.1)$$

(FMS =flowmeter percent reading)

Experimental discharge rates are less than the rates calculated from theoretical flow equations primarily because of the effect of internal molecular friction of the fluid and the viscosity. The theoretical flow equation is:

$$Q = A_w C_d \left[\frac{2gV_f(\rho_f - \rho_w)}{A_f \rho_w} \right]^{0.5} \qquad (B.2)$$

where Q=volumetric flowrate, A_w=cross-sectional area of the narrowest part of annulus, V_f=volume of float, ρ_f= density of float, A_f=cross-sectional area of the largest part of float, and ρ_w=density of fluid. The Coefficient of Discharge, C_d, is a function of viscosity. A constant value for C_d in equation (B.2) would be desirable as this would show a negation in the variations due to the viscosity. The effect of the float shape on C_d with varying Reynolds number is shown in Figure B.1 (a). The Reynolds number for the flowmeter uses an effective diameter of the tube inner diameter minus the float outer diameter. This plumb bob style float presents a large surface area to the fluid stream and the viscous effects increase as the flow rate increases. [Ref. 31: pp. 9804-9808]

The data collected from the calibration runs showed little or no change in the Discharge Coefficient over the 20 to 90 percent flowmeter setting range and the 15 K change in fluid temperature. The square edge plumb bob float reaches a constant Coefficient of Discharge at Reynolds

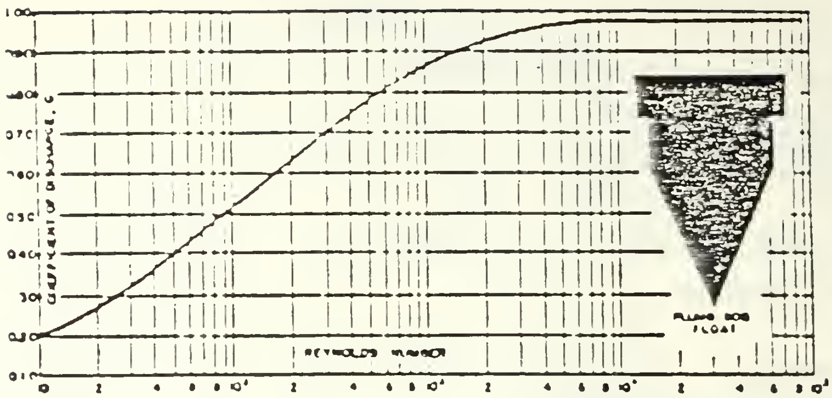

(a)

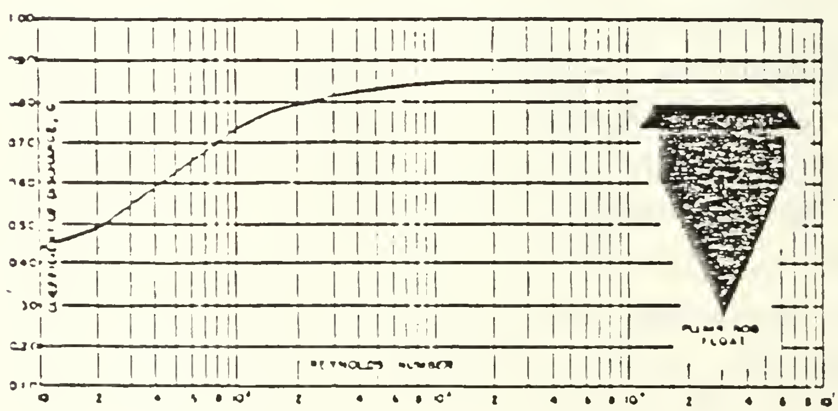

(b)

Figure B.1. Effect of Float Shape on Coefficient of Discharge: (a) Square Edge Plumb Bob Float (from Ref. 30), and (b) Taper Edge Plumb Float.

number > 10000. This is due to the effective shape of the float on the streamline pattern as shown in Figures B.2 (a) and (b). The experimental calibration range of 1300 < Re < 27000 displayed a flattening out of the Coefficient of Discharge. A different effective shape is seen by the streamline pattern because of the minimal clearances between the tube bead guides and the float. Also, the float used in this particular flowmeter had tapered edges versus square edges. This different effective shape is shown Figures B.2 (c) and (d). Figure B.1 (b) shows the effect of the float shape on the Coefficient of Discharge for the tapered edge float.

Additionally, the accuracy of the flowmeter contributes to the flattening effect on the Coefficient of Discharge shown by the experimental data. The accuracy effect is felt in two major components, reproducibility and scale factor. Reproducibility accuracy is minimally determined by the change in the fluid flowrate, corresponding float movement, and observation of float position. The calibration data had good reproducibility over the various flowrate and temperature ranges. The scale factor accuracy is inherent to the scale markings on the flow tube. Fischer Porter conducted numerous tests of flowmeter calibration readings. They used a maximum scale fraction error of 0.9 mm on a 250 mm tube. Based on their results, Fischer Porter reported [Ref. 31: pp. 9814-9816] an accuracy of plus or minus one percent at high flow rates was a reasonable expectation. Also, at low flow rates (< 20 percent) a resonable expectation would be an accuracy of eight to ten perecent.

The experimental data followed a trend of negligible viscosity effect. The flow tube design, float shape, and scale factor accuracy were the main contributors to this negation of a viscosity correction factor. As such, equation (B.1) was used without a viscosity correction factor to calculate the mass flowrate for the boiling tube runs.

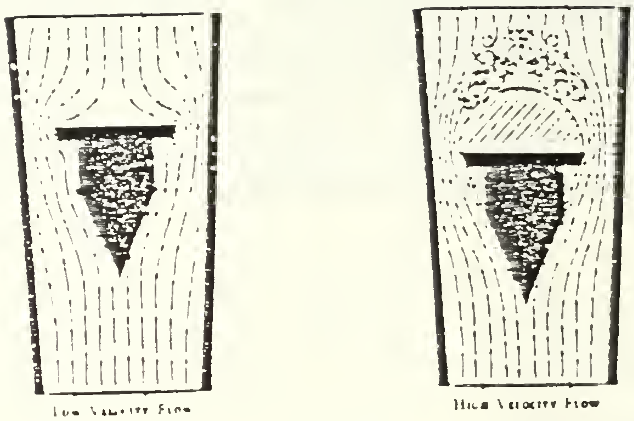

(a)

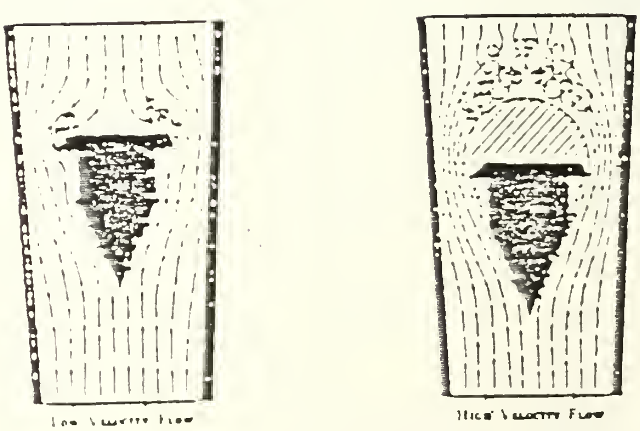

(b)

Figure B.2. Effect of Float Shape on Streamline Pattern: (a) Square Edge Plumb Bob Float (from Ref. 30), and (b) Taper Edge Plumb Bob Float.

APPENDIX C
MODIFIED WILSON PLOT

As referenced in Chapters III and IV, this appendix provides the data reduction procedures used to compute inside and outside heat-transfer coefficients. The tubes used for data collection were the smooth, modified High Flux, and Modified Turbo-B tubes. The modified Wilson plot anaylsis could not be directly run on the enhanced tubes since reliable boiling correlations for these surfaces do not exist. Also, only two unknowns can be allowed between correlations for the inside and outside heat-transfer coefficients. The steps used in this procedeure are outlined below and are contained in DRP4, which is cited in Appendix A:

Basic Equations

The overall heat-transfer coefficient in terms of the overall thermal resistance is given by:

$$\frac{1}{U_o} = \frac{A_o}{h_i A_i} + R_w + \frac{1}{h_o} \qquad (C.1)$$

where

$$R_w = D_o \ln\left(\frac{D_o}{D_i}\right) \frac{.5}{k_m} \qquad (C.2)$$

Modified Wilson Plot

1. Assume C_{sf} and T_f for the boiling side and compute:

$$\Omega = \left(\frac{c_p}{Pr^{1.7}}\right)^{\frac{1}{r}} \left[\frac{g(\rho_l - \rho_v)}{g_c \sigma_l}\right]^{0.5} \frac{\mu \Delta T^2}{h_{fg}^2} \tag{C.3}$$

$$h_o = \frac{\Omega}{\left(C_{sf}\right)^{\frac{1}{r}}} \tag{C.4}$$

Note: with r equal to 0.333, equation (C.3) represents the Rohsenow correlation [Ref. 23: p. 969].

2. Assume C_i and compute:

$$\Gamma = \frac{k}{D_i} Re^{0.8} Pr^{0.33} \left(\frac{\mu}{\mu_w}\right)^{0.14} \tag{C.5}$$

$$h_i = C_i \Gamma \tag{C.6}$$

3. Substitute h_o and h_i from steps 1 and 2 above into equation (C.1) and rearrange to yield:

$$\frac{1}{U_o} - R_w \Omega = \frac{A_o \Omega}{C_i A_i \Gamma} + \left(C_{sf}\right)^{\frac{1}{r}} \tag{C.7}$$

4. Now, let:

$$Y = \frac{1}{U_o} - R_w \Omega \tag{C.8}$$

and

$$X = \frac{\Omega A_o}{\Gamma A_i} \tag{C.9}$$

Construct the least-squares line for Y versus X in the form of:

$$Y = mX + C \tag{C.10}$$

5. Compute a new set of values for C_i and C_{sf} as follows:

$$C_i = \frac{1}{m} \tag{C.11}$$

and

$$C_{sf} = C^r \tag{C.12}$$

6. Repeat steps 1 through 5 until convergence for C_i and C_{sf} between two successive iterations is less than 0.1 percent.

APPENDIX D

DATA RUNS

The following table outlines the data runs used in this investigation:

Where:

1. WH - Smooth tube
2. HF- High Flux (i.e., porous-coated Korodense) tube
3. HFM - Modified High Flux (i.e., porous coating machined off) tube
4. TB - Turbo-B tube
5. TBM - Modified Turbo-B (i.e., external enhancement machined off) tube
6. T - inlet water temperature
7. V - water velocity
8. const - constant
9. dec - decreasing
10. inc - increasing

TABLE 4

DATA RUN DESCRIPTION

File Name	Oil %	# points	Description
WH01	0	10	Light Off Effect (cold water)
WH02	0	10	Light Off Effect (warm water)
WH03	0	9	Light Off Effect (steam)
WH05	0	10	T const V dec
WH06	0	8	T const V dec
WH07	1	10	T const V dec
WH08	1	10	T const V dec
WH09	2	10	T const V dec
WH10	2	10	T const V dec
WH10A	2	10	Repeatability WH10
WH11	6	10	T const V dec
WH12	6	8	T const V dec
WH13	6	8	Light Off Effect (warm water)
HF12	0	10	T const V dec
HF13	0	12	T const V dec Light Off Effect (steam)
HF14	0	12	Light Off Effect (cold water)
HF15	0	10	Light Off Effect (warm water)
HF16	0	12	Repeatability of HF12
HF22	0	7	T inc V const
HF23	0	6	T dec V const
HF24	1	12	T const V dec
HF25	1	10	T const V dec
HF26	1	6	T dec V const
HF27	1	7	T inc V const
HF28	2	12	T const V dec
HF29	2	12	T const V dec
HF30	2	6	T dec V const (Repeatability of HF28)
HF31	2	8	T inc V const
HF32	6	10	T const V dec
HF33	6	10	T const V dec
HF34	6	7	T dec V const
HF35	6	7	T inc V const
HFM01	0	8	Sieder-Tate Coeff Run
HFM02	0	8	Sieder-Tate Coeff Run
HFM03	0	10	Sieder-Tate Coeff Run
HFM04	0	8	Sieder-Tate Coeff Run
HFM05	0	8	Sieder-Tate Coeff Run
HFM06	0	8	Sieder-Tate Coeff Run
HFM07	0	10	Sieder-Tate Coeff Run
HFM08	0	8	Sieder-Tate Coeff Run
TB01	0	10	Light Off Effect (cold water)
TB02	0	10	Light Off Effect (warm water)
TB03	0	10	Light Off Effect (steam)

TB04	0	10	T const V dec (Repeatability of TB03)
TB05	0	6	T dec V const
TB06	0	10	T const V dec
TB07	0	7	T inc V const
TB08	1	10	T const V dec
TB09	1	6	T dec V const
TB10	1	10	T const V dec
TB11	1	6	T inc V const
TB12	2	10	T const V dec
TB13	2	10	T const V dec (Repeatability of TB12)
TB14	2	7	T dec V const
TB15	2	10	T const V dec
TB16	2	6	T inc V const
TB17	6	10	T const V dec
TB18	6	7	T dec V const
TB19	6	7	T inc V const
TB20	6	8	T const V dec Light Off Effect (steam)
TB21	6	10	Light Off Effect (cold water)
TB22	6	10	Light Off Effect (warm water)
TBM04	0	8	Sieder-Tate Coeff Run
TBM05	0	8	Sieder-Tate Coeff Run
TBM06	0	6	Sieder-Tate Coeff Run
TBM07	0	6	Sieder-Tate Coeff Run
TBM08	0	8	Sieder-Tate Coeff Run
TBM09	0	8	Sieder-Tate Coeff Run
TBM10	0	8	Sieder-Tate Coeff Run

APPENDIX E
UNCERTAINITY ANALYSIS

The uncertainity for mass flow rate, Reynolds number, heat flux, LMTD, wall resistance, overall heat-transfer coefficient, inside heat-transfer coefficient, and outside heat-transfer coefficient were analyzed for selected runs of the smooth, High Flux and Turbo-B tubes. The analysis was based on the Kline-McClintock [Ref. 32: p. 3] method of uncertainity analysis. For example, the following equations were used for the uncertainity of the heat flux:

$$q = \frac{Q}{\pi D_o L} \tag{E.1}$$

and

$$Q = \dot{m} c_p (T_{in} - T_{out}) \tag{E.2}$$

In accordance with Kline and McClintock, the uncertainities are given by:

$$\frac{\delta q}{q} = \left[\left(\frac{\delta Q}{Q}\right)^2 + \left(\frac{\delta D_o}{D_o}\right)^2 + \left(\frac{\delta L}{L}\right)^2\right]^{0.5} \tag{E.3}$$

and

$$\frac{\delta Q}{Q} = \left[\left(\frac{\delta \dot{m}}{\dot{m}}\right)^2 + \left(\frac{\delta c_p}{c_p}\right)^2 + \left(\frac{\delta T_{in}}{(T_{in} - T_{out})}\right)^2 + \left(\frac{\delta T_{out}}{(T_{in} - T_{out})}\right)^2\right]^{0.5} \tag{E.4}$$

The uncertainity in the conduction losses for the unenhanced ends of the boiling tube were considered negligible in comparison to the boiling surface uncertainity and as such, were disregarded. Table 5 lists the uncertainities for the previously mentioned values.

TABLE 5

UNCERTAINTY ANALYSIS PERCENTS

file	WH05	WH05	HF13	HF13	TB04	TB04
q (w/m)	31140	26690	49540	38780	68780	53670
V (m/s)	2.24	1.39	2.24	1.39	1.87	1.07
$\frac{\delta \dot{m}}{\dot{m}}$	1.56	2.51	1.56	2.51	1.43	2.51
$\frac{\delta Re}{Re}$	1.79	2.65	1.73	2.61	1.61	2.61
$\frac{\delta q}{q}$	1.59	2.52	1.59	2.52	1.46	2.52
$\frac{\delta LMTD}{LMTD}$	4.96	3.59	3.10	2.45	2.29	1.66
$\frac{\delta R_w}{R_w}$	2.76	2.76	11.17	11.17	2.92	2.92
$\frac{\delta U_o}{U_o}$	5.21	4.39	3.48	3.52	2.71	3.02
$\frac{\delta h_i}{h_i}$	2.03	2.56	1.61	2.25	1.48	2.21
$\frac{\delta h_o}{h_o}$	5.34	5.08	4.90	4.89	3.35	3.96

Note: All runs were performed in pure refrigerant
WH = Smooth tube
HF = Korodense tube with High Flux Coating
TB = Turbo-B tube

The large uncertainity for the wall resistance of file HF13 (porous- coated Korodense tube) is due to the 10 percent uncertainity of the thermal conductivity coefficient. For this investigation, the coefficient used was an average value for the values given in the open literature for copper-nickel plates or tubes.

APPENDIX F

LIST OF NOMENCLATURE

1. NOMENCLATURE

A - Surface Area

c_p - Specific heat at constant pressure

C_c - Oil concentration

C_i - Inside Sieder-Tate-type coefficient

C_{sf} - Rohsenow coefficient

d_i - Inside diameter of tube

d_o - Diameter of mouth of reentrant cavity

D - Diameter

e - Depth of internal ridge or fin

E_v - Energy transfer per unit volume

f - Friction factor

g - Acceleration due to gravity

g_c - Gravitational constant

h - Convective heat-transfer coefficient

h_{fg} - Specific enthalpy of vapor-liquid mixture

k - Conductive heat-transfer coefficient

k_m - Conductive heat-transfer coefficient of metal

L - Tube length

L_e - Entrance effect length

$\dot{m}$ - Mass flow rate

p - Distance between ridge or fin peaks

Pr - Prandtl number

q - Heat flux

Q - Total heat transfer

r - Tube radius

Re - Reynolds number

R_w - Thermal wall resistance

St - Stanton number

U_o - Overall heat-transfer coefficient

v_g - Specific volume of vapor

V - Velocity

Δ - Change (i.e., T_{in} - T_{out})

σ - Surface tension

σ_o - Surface tension of oil

σ_r - Surface tension of refrigerant

μ - Viscosity

μ_o - Viscosity of oil

μ_r - Viscosity of refrigerant

ρ - Density

ρ_o - Density of oil

ρ_r - Density of refrigerant

2. SUBSCRIPTS

f - fluid

i - inside

in - inlet

m - mixture

o - outside

ol - oil-liquid

out - outlet

rl - refrigerant-liquid

s - smooth tube

sat - saturation

w - water

wo - outside wall

LIST OF REFERENCES

1. Bergles, A. E. and Webb, R. L., "A Guide To The Literature on Convective Heat Transfer Augmentation," Advances in Enhanced Heat Transfer, Vol. 43, pp. 81-89, 1985.

2. Wanniarachchi, A. S., Marto, P. J., and Reilly, J.T., "The Effect of Oil Contamination on the Nucleate Pool-Boiling Performance of R-114 from a Porous-Coated Surface," ASHRAE Transactions, pp. 2-73, 1986 (accepted for publication).

3. ASHRAE Guide and Data Book, Chapter 18, pp. 281-291, 1963.

4. Dougherty, R. L. and Sauer, Jr., H. J., "Nucleate Pool Boiling of Refrigerant-Oil Mixtures From Tubes," ASHRAE Transactions, Vol. 80, pp. 175-178, 1975.

5. Chongrungreong, S. and Sauer Jr., H. J., "Nucleate Boiling Performance of Refrigerants and Refrigerant-Oil Mixtures," ASME Transactions, Vol. 102, pp. 701-705, November, 1980.

6. Fujii, M., Nishiyama, E., and Yamanaka, G., "Nucleate Pool Boiling Heat Transfer From Micro-Porous Heating Surfaces," Advances in Enhanced Heat Transfer, pp. 45-50, 1979.

7. Webb, R. L., "The Evolution of Enhanced Surface Geometries for Nucleate Boiling," Heat Transfer Engineering, Vol. 2, nos 3-4, pp. 46-69, Jan-June, 1981.

8. Reilly, J. T., The Influence of Oil Contamination on the Nucleate Pool-Boiling Behavior of R-114 from a Structured Surface, M. S. Thesis, Naval Postgraduate School, Monterey, California, pp. 30-35,65,70, March, 1985.

9. Czikk, A. M. and O'Neill, P. S., "Correlation of Nucleate Boiling From Porous Metal Films," Advances in Enhanced Heat Transfer, pp. 53-59, 1979.

10. Carnavos, T. C., "An Experimental Study: Pool Boiling R-11 With Augmented Tubes," Advances in Enhanced Heat Transfer, pp. 103-108, 1981.

11. Czikk, A. M., Gottzmann, C. F., Ragi, E. G., Withers, J. G., and Habdas, E. P., "Performance of Advanced Heat Transfer Tubes in Refrigerant-Flooded Liquid Coolers," ASHRAE Transactions, Vol. 76, part 1, pp. 96-107, 1970.

12. Arshad, J. and Thome, J. R., "Enhanced Boiling Surfaces: Heat Transfer Mechanism Mixture Boiling," ASME-JSME Thermal Energy Engineering Joint Conf., Vol. 1, pp. 191-197, 1983.

13. Arai, N., Nakajima, T., Fukushima, T. Fujie, K. Arai, A., and Nakayama, Y., "Heat Transfer Tubes Enhancing Boiling and Condensation in Heat Exchangers of a Refrigerating Machine," ASHRAE Transactions, Vol. 83, part 2, pp.58-62, 1977.

14. Ayub, Z. H. and Bergles, A. E., "Pool Boiling from Gewa Surfaces in Water and R-113," Augmentation of Heat Transfer in Energy Systems, Vol. 52, pp. 57-64, 1985.

15. Nakayama, W., Daikoku, T., Kuwahara, H., and Nakajima, T., "Dynamic Model of Enhanced Boiling Heat Transfer on Porous Surfaces," Advances in Enhanced Heat Transfer, pp. 31-43, 1979.

16. Jensen, M. K. and Jackman, D. L., "Prediction of Nucleate Pool Boiling Heat Transfer Coefficients of Refrigerant-Oil Mixtures," ASME Transactions, Vol 106, pp. 184-190, 1984.

17. Marto, P. J., Reilly, D. J., and Fenner, J. H.; "An Experimental Comparison of Enhanced Heat Transfer Condenser Tubing," Advances in Enhanced Heat Transfer, pp.1-8, 1979.

18. GA Technoligies Report, GA-A17833, Fluid Mechanics and Heat Transfer Spiral Fluted Tubing, by J. S. Yampolsky et. al., 1984.

19. DSR Report, 70790-69, Investigation of Heat Transfer Augmentation Through Use of Internally Finned and Roughened Tubes, by A. E. Bergles et. al., pp. 18-23, 1970.

20. Karasbun, M., An Experimental Apparatus to Study Nucleate Pool Boiling of R-114 and Oil Mixtures, M. S. Thesis, Naval Postgraduate School, Monterey, California, pp. 24-32, 54-56, December, 1984.

21. Chaddock, J. B., "Influence of Oil Refrigerant Evaporator Performance," ASHRAE Transactions, Vol. 82, part 1, pp. 474-486, 1976.

22. AERE Report, R7318, The Development of Heat Transfer Tubes, by I. H. Newson and T. D. Hudgson, 1973.

23. Rohsenow, W. M., "A Method of Correlating Heat Transfer Data for Surface Boiling of Liquids," ASME Transactions, Vol. 74, p.969, 1952.

24. Incropera, F. P. and DeWitt, D. P., Fundamentals of Heat Transfer, John Wiley and Sons, p. 406, 1981.

25. Withers, J.G., "Tube-side Heat Transfer and Pressure Drop for Tubes Having Internal Helical Ridging with Turbulent/Transitional Flow of Single-phase Fluid: Part 1--Single-helix Ridging," Heat Transfer Engineering, Vol 2, No. 2, 1980.

26. Withers, J. G., "Tube-side Heat Transfer and Pressure Drop for Tubes Having Internal Helical Ridging with Turbulent/Transitional Flow of Single-phase Fluid: Part 2--Multiple-helix Ridging," Heat Transfer Engineering, Vol 2, No. 2, 1980.

27. Nobukatsu, A. and et. al., " Heat Transfer Tubes Enhancing Boiling and Condensation in Heat Exchangers of a Refrigerating Machine," ASHRAE Transactions, Vol. 83, part 2, pp. 58-70, 1977.

28. Green, G. H., "Influence of Oil on Boiling Heat Transfer and Pressure Drop in Refrigerants 12 and 22," ASHRAE Journal, pp. 57-61,1982.

29. Stephan, K., "Influence of Oil on Heat Transfer of Boiling Freon 12 (Refrigerant 12) and Freon 22 (Refrigerant 22)," Proceedings of XIth International Congress of Refrigeration, Vol. 1, pp. 369-379, 1963.

30. Stephan, K., and Mitrovic, J., "Heat Transfer in Natural Convection Boiling of Refrigerant-Oil Mixtures," Models and Correlations Review, pp. 73-85, 1982.

31. Fischer and Porter Company, Theory of the Flowrator, Catalog Section 98-A, pp. 9801-9816, 1947.

32. Kline, S. J. and McClintock, F. A., "Describing Uncertainities in Single-Sample Experiments," Mechanical Engineering, p. 3, Jan. 1953.

INITIAL DISTRIBUTION LIST

		No. Copies
1.	Library Code 0142 Naval Postgraduate School Monterey, California 93943	2
2.	Defense Technical Information Center Cameron Station Alexandria, Virginia 22314-6145	2
3.	Department Chairman, Code 69 Department of Mechanical Engineering Naval Postgraduate School Monterey, California 93943	1
4.	Professor Paul J. Marto, Code 69 Mx Department of Mechanical Engineering Naval Postgraduate School Monterey, California 93943	3
5.	Dr. A. S. Wanniarachchi, Code 69Wa Department of Mechanical Engineering Naval Postgraduate School Monterey, California 93943	2
6.	Dr. B. H. Hwang, Code 2722V David W. Taylor Naval Ship Research and Development Center Annapolis, Maryland 21402	1
7.	Mr. R. Helmick, Code 2745 David W. Taylor Naval Ship Research and Development Center Annapolis, Maryland 21402	1
8.	Mr. N. R. Clevinger Product and Process Development Mgr. Wolverine Tube P. O. Box 2202 Decatur, Alabama 35602	1
9.	Mr. J. McManus Box 139 Logan Lake, British Columbia Canada V0K 1W0	1
10.	Lt. S. McManus 6840 N. Columbus Blvd Tucson, Arizona 85718	2
11.	Mr. Elias Ragi Union Carbide Corporation P. O. Box 44 Tonawanda, New York 14151	1
12.	Dr. Masafumi Katsuta School of Science and Engineering 3-4-1, Ohkubo, Shinjukuku, Tokyo, 160, Japan	1

219549

Thesis
M2537
c.1

McManus
Nucleate pool-boiling of R-114 refrigerant and oil mixtures from water-heated enhanced surfaces.